BRNO UNIVERSITY OF TECHNOLOGY

Faculty of Mechanical Engineering

Institute of Machine and Industrial Design

Ing. Michal Michalec

PERFORMANCE AND SAFETY IMPROVEMENT OF LARGE-SCALE HYDROSTATIC BEARINGS

NAVÝŠENIE VÝKONNOSTI A BEZPEČNOSTI VEĽKOROZMERNÝCH HYDROSTATICKÝCH ULOŽENÍ

Shortened version of PhD Thesis

CONTENTS

1 INTRODUCTION

Hydrostatic (HS) lubrication principle was firstly introduced in 1852 by L. D. Girard. Since Rowe patented the HS bearing in 1985, the interest in HS lubrication research has been rising over the years. The HS lubrication principle is based on supplying pressurized fluid into HS pad to separate solid bodies and create thick lubricating film; thus the bearing can be operated even when standstill. HSB are key parts of machines requiring long durability, minimum downtime, and smooth and precise movement. This type of bearing can be used in a wide range of applications – from small millimetre-sized spindles up to large-scale machines and structures exceeding tens of metres.

With the increasing demand for large-scale machines of high precision, HS lubrication regime offers huge scalability. Compared to rolling bearings HSB can be utilized for moving structures exceeding tens of metres while keeping relatively high precision. Achieving high precision with rolling bearings at large scales would lead to extremely increased costs, while the HS lubricating film can even work properly with certain magnitude of surface error that is compensated with changing the hydraulic circuit performance. Another issue emerges with rolling elements wear that leads to necessary service. Moreover, HSB can be operated at low-speed and even in stationary conditions, unlike hydrodynamic or rolling element bearings working in elastohydrodynamic lubrication regime.

HSB offer long durability, minimal downtime, and high precision. However, large-scale HSB encounter issues with the manufacturing precision and challenging manipulation. Therefore, HSB is usually divided into smaller segments to simplify manufacturing, transport, and assembly processes. This might generate problems linked with the assembly precision of the segmented sliders and misalignment of the bearing pads. Moreover, the electricity consumption of the HSB pump required for proper operation is proportionally rising with its size, thus it is necessary to reduce the energetic demands and electricity consumption.

2 STATE OF THE ART

L. D. Girard opened new possibilities in the mechanical engineering industry by the introduction of water-fed bearings in 1852. The development process has advanced enormously ever since. Reynold's publication on the theory of lubrication [1] based on Tower's discovery of the hydrodynamic lubrication in 1886 significantly contributed to the fluid flow understanding. In 1918, Lord Rayleigh [2] discussed the optimal step bearing geometry for maximum load capacity, now referred to the Rayleigh step bearing. In the next period, the development process and application of externally pressurized bearings were continuously growing, numerous patents were proposed, and hydrostatic bearings were introduced in a separate chapter of a book by Khonosari and Booser [3] in 1970. A review paper on hydrostatic and hybrid bearings was presented by Rowe [4] in 1989 that summarized previous advances in this field. Later in 1992, Bassani and Piccigallo [5] wrote a comprehensive book describing all the important aspects of the hydrostatic bearing design and optimization based on the latest research. Research progress in the field of large hydrostatic bearings was further reviewed by Li et al. [6] in 2014. Later, an insight into hydrostatic bearing system research and applications was presented by Liu et al. [7], proving that hydrostatic lubrication was still an increasingly significant topic. Despite all the previous significant contributions in the field of hydrostatic lubrication, the latest technology developments offer new opportunities for further hydrostatic bearing improvement.

Hydrostatic lubrication works on the principle of feeding pressurized fluid in between sliding surfaces to secure their separation [5] as shown in Figure 1. The fluid is supplied from a hydraulic circuit through an inlet hole and evenly distributed by a recess. The turntable is floating and is ready for operation once the lubricating film is fully developed. The fluid pressure is gradually decreasing from the recess area to the atmospheric pressure, and the outlet fluid is collected and returned to the circulation.
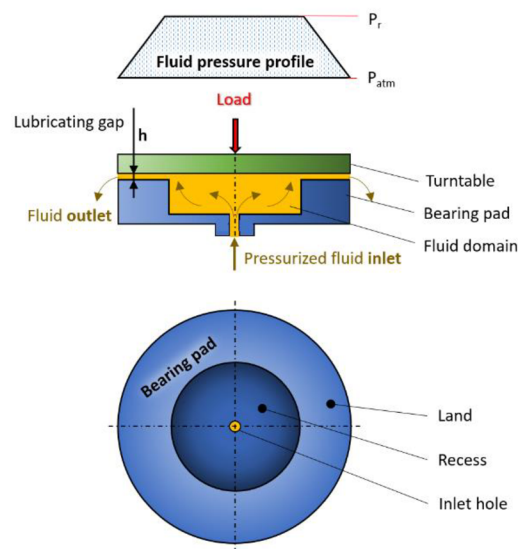

Figure 1 Schematic representation of the open-type hydrostatic bearing pad and fluid pressure distribution.

The main advantages of the hydrostatic bearing are very low friction only generated by the fluid shear forces and almost no wear of sliding surfaces that are completely separated by pressurized fluid film. The bearing is working even when standstill because the surface separation is maintained externally. Since the bearing clearance is filled with the pressurized fluid, the hydrostatic bearing shows a high damping ability and high stiffness while the noise emission and vibration transfer is very low. Because of solid contact absence, the hydrostatic bearing exhibits very high moving accuracy and stability without any undesirable stick-slip effect [8], [9]. Nevertheless, there are also several disadvantages that must be considered before selecting the hydrostatic bearing for a specific application. High precision of sliding surfaces is required; thus, the initial manufacturing costs can be considerably higher. The initial cost is increased by the necessity of an external pressurized fluid supply, considering all the elements of hydraulic circuit needed for proper functioning. Considering the complexity of the hydrostatic bearing system, a greater space is required for piping, hydraulic and electric energy supply compared to other types of bearings. Despite the low noise emission generated in between the sliding surfaces, the hydrostatic bearing system noise emission generated by the motor of the pump should not be overlooked. However, the noise transmitted by air, fluid, and structure [10] can be reduced by insulating material or by hydrogenerator confinement in an insulated space. The fluid-transmitted vibrations [11] can be dampened by the hydraulic accumulator [12], while structural vibrations can be reduced using silentblocks or shock absorbers.

Large-scale bearings are fundamental supporting elements of heavy rotary parts. The use of rolling elements is limited by the maximal diameter and load capacity. The size of rolling bearings is mostly only a few millimetres. However, large rolling bearings for wind turbines can reach 5 m [13]. The issue with large rolling bearing is not only the size and required precision of rolling elements, but also fatigue [14] and raceway/ball damage due to high contact stress [15]. In contrast to the rolling bearings, the hydrostatic bearings are beneficial for their applicability in wide constructions, large load carrying capacity, and uniform stress distribution. Hence, the hydrostatic bearings have been used for large tunnel drilling machines [16], large ship shafts and journal bearings [17], thrust bearings [18], and antenna or telescope structures carrying and operation, such as Giant Magellan telescope [19], [20]. Possibly, this type of bearing can be used for large ships propellers, crushing machines, large rotating blades [16], heavy transportation turning, or stage and assembly line manipulation and accurate positioning. Another important application of hydrostatic bearings are CNC turntables for dimensional workpieces [21], and dampers [22], [23] thanks to the characteristics of fluid during compression, and impact loading and vibration damping. One of the most significant uses of hydrostatic bearings is hydropower units [24]; when the hydroelectric turbine [25] of the hydrogenerator [26] needs to start spinning without contacting surface damage, the hydrodynamic (HD) bearing is combined with hydrostatic bearing pockets [27], when a hybrid bearing is started, stopped, or reversed without damaging the contacting surfaces of the bearing. Moreover, the high load and the possibility of pumping water is advantageous for ship sealift lock-gate hinge where the sea level difference needs to be overcome [28]. Additionally, the

working principle can be used for a rotary recovery device for the desalination process and reverse osmosis [29]. As introduced above, hydrostatic bearings have a great application potential that will be increasing with the development of modern technologies and trends [30], such as Industry 4.0 [31].

2.1 Overview of a large hydrostatic bearing system

In the case of large-scale bearings, manufacturing, transportation, and assembly have become one of the most important criteria in the design process. The hydrostatic pad can be either uniform, assembled from ring segments, or divided into separate segments supporting the turntable. Uniform hydrostatic pad (single pad bearing – *Figure 2* a**)** is advantageous in the height positioning of turntable segments. However, the manufacturing and transportation process can be much more complicated compared to the other geometry type. Additionally, discharge grooves for hydrostatic recess separation (*Figure 2* b) are recommended to avoid mutual recess flow interference [35]. Separated hydrostatic pads (multi pad bearing – *Figure 2* c) are preferred for simpler manufacturing and transportation. Moreover, the manipulation throughout the assembly process is greatly improved. Nevertheless, levelling and positioning is more difficult than in the uniform hydrostatic pad.
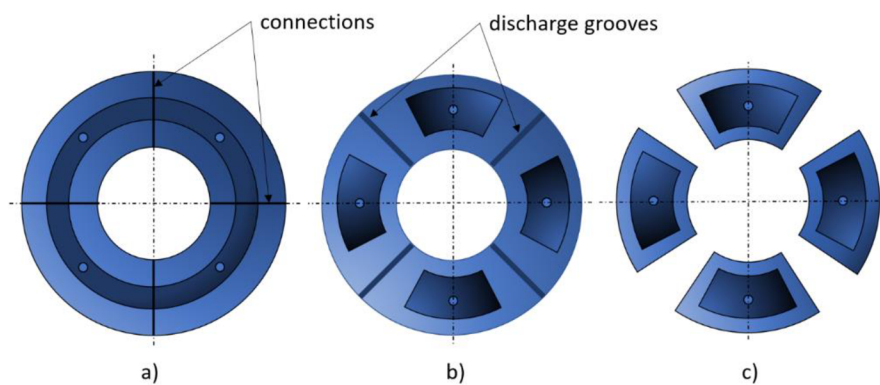

Figure 2 The geometry of a) single-pad single-recess, b) single-pad multi-recess, and c) multi-pad hydrostatic bearing types.

A full scheme of a large-scale hydrostatic bearing is shown in *Figure 3*. The hydrostatic bearing is composed of two main sections: the hydrostatic pad and the hydraulic circuit. The hydrostatic pad is a stationary part supporting the rotating turntable with load. The second fundamental part of hydrostatic bearing is the hydraulic circuit. A constant flow supply system has a separate hydrogenerator for each recess; however, supplying many recesses would be a complication because of either space or initial costs. Therefore, the multi-pad hydrostatic bearing is supplied by one pump with flow dividers and restrictors [33]. Moreover, large hydrostatic bearings are limited by manufacturing, transportation, and assembly processes, so those types of bearings are frequently composed of a large ring with numerous inlets [36] or numerous pads placed in a desired bearing diameter [37]. The pump supplies the hydrostatic pad with enough pressurized fluid at a higher pressure than required by the pad; thus, the flow volume and pressure is processed using hydraulic valves. Three types of hydraulic valves are included: way-valves to control direction of oil flow, pressure control valves to control pressure in different segments in the circuit, and flow control valves to control the flow rate in the circuit.

Flow control valves are especially important components of the hydrostatic bearing because they maintain constant film thickness by compensating pressure differential during impact and non-symmetric loading and vibrations. The hydraulic accumulator acts as a fail-safe measure in case of sudden hydraulic circuit failure.
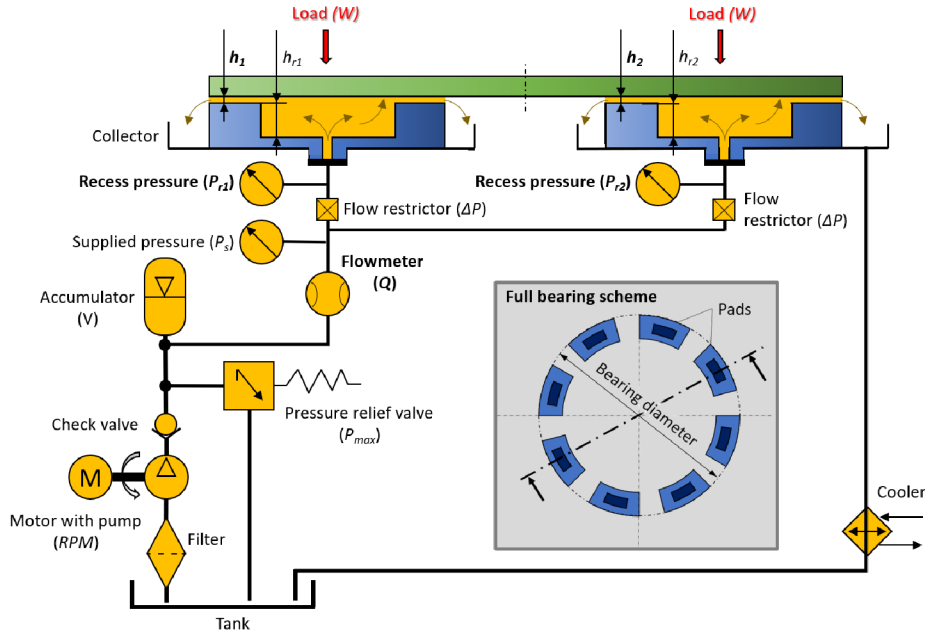

Figure 3 Full scheme and cross section of two hydrostatic pads of a large multi-pad hydrostatic bearing.

2.3 Calculation and optimization

Basic requirements for flow investigation in a narrow gap are isotropic and continuous conditions in an elementary volume. Thus Navier—Stokes equation can be used for viscous fluid flow description in eqn. (1).

$$\rho \frac{Dv}{Dt} = \rho f + \nabla \sigma \qquad (1)$$

However, the complexity of Navier—Stokes equations may be reduced by applying such simplifications as averaging quantities along one direction, flow linearity and inertia terms [5]. Thus, the Reynolds equation without viscosity variations can be derived as shown in eqn. (2).

$$\nabla \left(\frac{h^3}{\eta} \cdot \nabla \vec{p} \right) = 6 \nabla (\overrightarrow{U \cdot} h) + 12 \frac{\partial h}{\partial t} \qquad (2)$$

Alternatively, the complexity of Navier—Stokes equations can be reduced into a 2D problem using the Dirichlet conditions [38] to obtain analytical formulations. Bassani and Piccigallo [5] derived simple-pad and single-recess geometry, such as circular, rectangular, and annular. Several other configurations for multi-recess bearings were introduced by Khonosari and Booser [3]. These are based on pad coefficients, whose values are selected from a graph. In Table 1 equations for circular pad are expressed, showing the key parameters of a hydrostatic bearing.

Table 1 Example of expressed equations for circular hydrostatic pad calculation [3], [5], [39]

Quantity	Equation
Required lifting pressure in recess area	$p_r = \dfrac{W}{A_{min}}$
Total load-carrying capacity	$W = 3\dfrac{\mu r_2^2}{h^3} Q \left(1 - \dfrac{r_1^2}{r_2^2}\right)$
Flow rate	$Q = \dfrac{\pi h^3 p_r}{6\mu ln(r_2/r_1)}$
Viscous friction	$\tau = \dfrac{\pi \mu \omega}{2h}(r_2^4 - r_1^4)$
Fluid power loss	$H_v = \omega \tau$
Pumping power loss	$H_p = p_r Q$

To evaluate the performance of a non-derived hydrostatic bearing shape analytically, an approximation method according to Rippel [40] can be utilized to obtain roughly corresponding load capacity. Calculation generalization was introduced using performance parameters as introduced by Khonosari and Booser [3] to simplify the design process for derived geometry hydrostatic bearing shapes as shown in eqn. (3).

$$W = A_{eff} \cdot p_r = a_p \cdot A_{tot} \cdot p_r \qquad (3)$$

where A_{eff} is the effective area of a pad, A_{tot} is the total pad area, and a_p is the pressure coefficient. This form is advantageous for the application of results from the numerical simulation resultant forces [35] and for obtaining of pressure coefficients for a specific geometry. The analytical calculation process is performed using analytical expressions for the determination of basic parameters and required hydropower unit performance. The numerical approach serves as an auxiliary tool for performance optimization and deformation investigation, which is discussed in this paper in detail later. A summary of both analytical and computation approaches is listed in Table 2. Numerical methods can be implemented in the hydrostatic bearing design to achieve desired performance and eliminate possible issues in advance. The computational fluid dynamic (CFD) is a powerful tool for fluid flow simulation and investigation.

Table 2 Comparison of analytical and numerical approaches in hydrostatic bearing calculation

Analytical	Numerical
Simple and quick calculation of key parameters.	Required advanced knowledge of fluid modelling.
Can be used for [5]: - static and dynamic performance analysis, - thermal and flow properties prediction, - optimization of basic shape pads using, nomographs.	Can be used for: - static and dynamic performance analysis [41], [42], - flow investigation [43], [44], - thermal properties evaluation [45], [46], - deformation evaluation [24], [47], - error modelling [48]–[50].
Preferred for basic derived pad geometry shapes.	Powerful tool for obtaining resultant force for various pad and recess geometry from simulation [29], including unusual shapes.
Limited to simple geometry configurations.	Suitable for unusual configurations of recess and pad shapes design that is very difficult or impossible to express analytically [51].

2.4 Performance optimization

Performance optimization is an important process that includes both optimal control establishment and the whole system energy consumption minimization. The hydrostatic bearing performance is provided according to a selected design criterion as listed in **Chyba! Nenalezen z droj odkazů.**. Simple cases deal only with the optimization of one parameter, which is, however, not enough for obtaining high performance, good thermal properties, and economical energy management. Therefore, a multicriteria optimization was introduced by Solmaz et al. [52] as an iterative process considering the most important parameters, specifically minimum power, and temperature rise. The better required overall performance, the more criteria should be considered. A remarkable 30-60% accuracy [53] can be achieved by considering the influence of design parameters, geometric errors, deformation, temperature, and random parameters. Fedorynenko et al. [54] proposed an innovative design of hybrid bearing achieved a significant efficiency increase, i.e. 1.5 times decreased total energy loss in hydrostatic mode and 4 times in HD mode.

2.5 Pad geometry optimization

The bearing pad recess area provides enough lifting force to the bearing turntable and load. Additionally, the recessed pad has significantly better performance compared to a non-recessed pad [61], [62], allowing the bearing to withstand higher rotating speeds and load variations. However, different recess shapes exhibit slightly different characteristics. Generally, mostly preferred are conventional shapes [63], such as circular, rectangular and annular, because of derived equations and manufacturability. With the advancement of computational software and manufacturing technologies, triangular and elliptic [64], or even unconventional geometry shapes [65] can be developed.

A lifting pocket can also be included in a HD bearing design. For instance, the results of numerical investigation of the recess presence by Fillon et al. [66] showed a plateau, a less contrasted distribution, in the pressure field and a small decrease in the temperature field. Thus, the performance of hybrid bearings is improved with the recess presence, while the thermal properties are preserved or slightly enhanced. On the contrary, Wasilczuk et al. [67] observed in field tests, the hybrid bearing maintains a higher film thickness and lower temperature rise, but also greater friction losses due to larger viscosity of oil with lower temperature. The ration of the hydrostatic pad recess area to the total pad area plays a significant role in the overall performance of the hydraulic supply. For a single recessed hydrostatic pad, the optimal ratio values for circular, annular, and square shapes range from 0.4 to 0.6 [5], depending on the recess outline shape. The outside dimensions of a rectangular pad and the optimal ratio of recess dimensions for best damping and stiffness characteristics were found to be 1 [68], thus the square shape is superior to the rectangular one in terms of required performance. The higher the pocket ratio, the better static and dynamic performance of the pad can be achieved. Yet, higher

pumping performance is necessary. However, in case of lower pocket ratios [69], in the range of 0.1-0.4, larger frictional power loss occurs.

The recess depth also plays an important role in the bearing performance. Common design practice for a recess depth design [70] is 50-100 times the expected film thickness. However, for highspeed thrust bearings, the optimal recess depth can be rather smaller, below 25 times the expected film thickness. Horvat and Braun's [71] investigation of two-dimensional flow visualisation with an experimental verification confirmed that at low-speed operation the Poiseuille pressure forces dominate, while at high speed the Couette shear forces become more influential. The results clearly show that the pressure forces are dependent on the rotation direction, creating a combined effect at one side of bearing and a counteracting effect at the opposite. Shen et al. [72] investigated a three-dimensional flow, contributing to the increased precision of heavy-duty hydrostatic bearing performance prediction. For very shallow recess with a depth less than 2 mm [73], the dynamic pressure significantly increased even at the low rotational speed of 6 rpm. Recess depths above 2 mm showed constant values of pressure. Tian et al. [74] investigated inertia effects and couple stress in numerical simulations, concluding that the recess depth affects static properties of hydrostatic thrust bearings, while noticing that a recess depth higher than four times the film thickness showed a negligible effect on the performance. Yu et al. [75] confirmed that the dynamic pressure rise in shallow recess depth is stronger at higher speeds. For heavy bearings operating at 80 rpm [76], the recess depths above 3 mm showed constant oil film pressure, thus the higher the speed, the higher pressure and stiffness can be achieved. However, it is not possible to establish an optimal depth without expected film thickness, and therefore Helene et al. [77] proposed recess depth to film thickness ratio H1/H2 for laminar and turbulent flow regimes, where deep pockets (H1/H2 > 16) show a constant pressure level for both regimes.

2.6 Sliding surfaces

The requirements on sliding surfaces of hydrostatic bearings are relatively high due to a small gap in maintained by pressurized fluid. Therefore, a precise design and analysis are necessary to avoid any unwanted collisions caused by unexpected thermal or structural deformations, and errors created during the manufacturing and assembly processes.

2.6.1 Structural deformation analysis and prevention

The lubricating film thickness between the sliding surfaces ranges between hundreds and tens of microns [36], [78], so the potential deformations must be considered in advance. Modern software offers great support to the design process by simulations, either structural or fluid. Two main components generating structural deformations are a deformation of the turntable caused by mechanical load when the increasing load causes deformation of the turntable [79] and a thermal deformation of the turntable caused by insufficient lubricant cooling or excessive heating at choking elements or at the inlet into the hydrostatic pad [80]. Elastic and thermal distortion effects directly affect the load and error acceptance range [34]. Numerical methods play an important role during this stage of the development process. Using the FVM and FSI, it is possible to predict the fluid film interface deformation caused by loading [81] or the

temperature field of tilted sliding surfaces [59] because of asymmetric loading or inaccurate assembly.

2.6.2 Manufacturing and assembly error analysis and prevention

The very thin lubricant film thickness has demanding requirements on the sliding surface precision. The increase of pressure in the recess raises the value of lubricating film thickness only slightly while increasing the required performance strongly. Therefore, it is necessary to achieve a high precision of sliding surfaces. Thermal changes and load effects of machining tools during the manufacturing process always influence the proportions of geometrical errors. Besides structural and thermal deformations, other errors are generated during the manufacturing and assembly.

The main geometric accuracy parameters [34] are cylindricity and flatness [82] for radial and thrust bearings respectively. Manufacturing errors of radial bearings was investigated by Rajput and Sharma [83] numerically, based on the Reynolds equation, to clarify the combined influence of geometric imperfections and axis misalignments on the minimum film thickness for barrel, bellmouth, and undulated journal shapes. Waviness modelling can be related to surface roughness as well. Large-scale bearing mounting encounters complications connected with the inaccuraccy of their foundations. Therefore, additional measures for proper positioning are necessary. Error compensation proposed by Zha et al. [49] based on a laser interferometer provides a timely effective measurement process, but not greatly suitable for large turnables. A different approach to measuring is photogrammetry [84] that has previously been used for large sites, (as large as 10—20 m with only 10—26 mm error). Its main advantage is the simplicity of the measurement system and portability. However, the required precision for assembly error of large hydrostatic bearings might not be satisfactory and nowadays can only be used for partial measurements. A frequently used mechanism for uniform hydrostatic pad leveling was introduced by Johns et al. [20] in the Giant Magellan Telescope design where there are adjustment screws between track and pier (*Figure 4*). The leveling compensation of hydrostatic Lock-gate proposed by Ostayen et al. [85] was based on rubber support. The use of such support is possible for stable and lower ambient temperatures because the elastomer material aging process [86], [87] at temperatures above 70 °C decreases the rebound resilience, tensile strength, and elastic modulus, while the hardness increases. Higher temperatures can eventually lead to swelling [88] and an increase in the volume of up to 2.4 times.
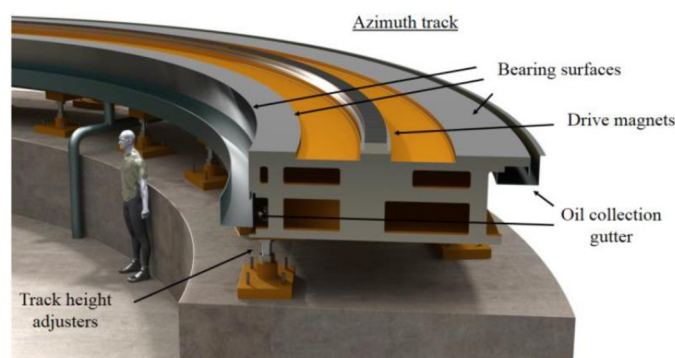

Figure 4 Azimuth track of the Giant Magellan Telescope (reprinted from [20] with permission from SPIE).

2.7 Hydrostatic bearing supply system

The hydraulic circuit is the second, equally important part of the hydrostatic bearing. A pressurized fluid supply is necessary for proper working of the hydrostatic lubrication. Preferably, the design process of the hydraulic circuit is defined by performance requirements. With respect to large dimensions and numerous hydrostatic pads required to supply with pressurized fluids, the use of flow compensators is necessary and will be described in detail in the following chapter.

2.7.1 Flow compensation

In case of large hydrostatic bearings, several hydrostatic pads are usually used due to the previously stated limitations; a compensating device is necessary for maintaining a constant lubricating film thickness. There are several ways of the pressurized fluid distribution into individual hydrostatic pads. There are numerous options of flow control compensation devices available, all described in a comprehensive summary in [89]. Restrictor types can be divided according to geometry into fixed or variable. An unusual restriction type was proposed by Xu et al. [90] where a combination of numerous orifice restrictors in the hydrostatic hinge inner compensation led to significantly better performance than only orifice-compensated hydrostatic hinge. Nonetheless, the latest trends in flow compensation aim at intelligent control [91] to maximize the performance and cut down friction losses. A particularly important advancement in flow control is variable viscosity monitoring [92] according to actual oil temperature in the recess to avoid the loss of a load-carrying capacity due to lubricant overheating.

2.7.2 Accumulator units

Accumulator units serve as temporary supply of pressurized fluid in the hydraulic circuit, for example in case of hydrogenerator supply failure [93], making it an important element for sliding surface damage. The accumulator price is a small sacrifice considering costly maintenance and repairs [94] that could emerge from electricity drop-out and other possible disturbances. Hydraulic accumulators are often connected with energy recovery systems and energy transformation [95]. However, they also play an important role in energy saving and storage [96], pressure fluctuation reduction [97], and shock absorbing element in fast heavy forging machines [98]. As observed by Xue et al. [50], the fluctuation of the supply pressure increases the linear motion errors. Moreover, inclusion of hydraulic accumulators leads to pulsation pressure reduction. Besides the fail-safe measures, accumulator units can be helpful for thermal expansion and leakage compensation in extreme conditions [96], considering relatively small changes in the pressure at a wide range of volume increase.

2.7.3 Lubricants

As previously mentioned, lubricant characteristics directly influence the overall performance of the hydrostatic bearing. Viscosity-pressure dependence is normally not considered even though liquids under extreme pressure often show an increase in viscosity, thus only the pumping performance will be affected. The viscosity-temperature dependence is far more important since the pump and choking members generate heat. An unexpectedly high temperature rise could even lead to a serious decrease in load-carrying capacity [99] and

eventually to a loss of the load-carrying ability. To achieve a higher calculation accuracy, a variable viscosity should be considered [100], while an expected ambient temperature range and internal fluid heating on choking elements must be included in the design stage. Mostly used lubricants are oils because of certified classification of viscosity index (VI) according to ISO VG. Mineral oils are of satisfactory performance and relatively reasonable price. ISO VG 10/15/22/32/46/68/100/150 are chosen according to expected working and surrounding temperatures, and the hydrogenerator performance. Oils of these grades are advantageous due to low friction performance and a neutral effect on sealing elements. For specific environments other fluids could be used, based on their applicability and suitability. An example is water [47], [101] and saltwater [85], [102] that are beneficial for use in mechanism manipulation with a difficulty of oil sealing. However, in such aggressive conditions, materials must be carefully selected and treated [103].

3 SUMMARY AND CONCLUSIONS OF STATE OF THE ART

HS lubricating film is created between sliding surfaces by an external hydraulic supply. It secures complete separation of the conformal surfaces, resulting in very low friction, almost no wear, very high precision without occurrence of stick-slip effect, high stiffness and vibration damping ability. The use of fluid bearings might lead to higher energy efficiency compared to rolling or sliding bearings with direct contact [13], even though HS lubrication requires continuous external supply of pressurized lubricant. HS lubrication is a unique type of lubrication regime that is suitable for a wide range of applications – from millimetres up to tens of metres [2] – for small high precision bearings, through medium-sized machining centres, or even for moving large structures, such as giant telescopes, radio antennas, or large-scale machining centres. In the case of large-scale applications, the slider and pad bodies are not possible to be manufactured in one piece, because of manufacturing space, transportation, and assembly. The performance, precision, and safety of large-scale HSB can be heavily influenced by assembly precision, which has not yet been specified in the available literature. Moreover, HSB require pressurized oil supply for proper function, therefore the energetic demands for operation are higher than other types of bearings, thus energy consumption should be minimized as much as possible. A comprehensive methodology on HSB design and optimisation was published by Bassani & Piccigallo [14]. This book provides a strong foundation for HSB design engineers. Nonetheless, some of the challenges and issues that are linked with large-scale machines and structures show new challenges and issues, especially regarding assembly precision and the use of computational software for bearing geometry optimization, which has been remarkably improved over the last few years.

Bearing safety

Geometric errors negatively influence the lubricating layer of sliding bearings, whose performance is decreasing with the magnitude of surface irregularities [15]. Misalignment in hydrodynamic (HD) bearings is strongly influencing the lubricating film. HS bearings are often combined with HD bearings to reduce wear during start and stop phase [16], and compensate misalignment and are frequently mounted on tilting support of the pad [17]. HS lubrication regime increases the film thickness and improves lubricant circulation and cooling [18], thus improving its performance. This is one of the main reasons why HS lubrication is used for bearings of high-precision machines. Nonetheless, HS bearings have also certain limits to compensate the geometric errors. The energetic demands needed to compensate the geometric precision of the solid bodies surrounding the lubricating film [19] are rising with the error magnitude. An unconventional way of error compensation, by using compliant members was employed for slider surface [20] and pad support [21]. The previous research was aimed at the pad misalignment compensation modelling using compliant support numerically [22]. Numerical modelling was also used for geometric error investigation. Model for motion error analysis of closed guideways lubricated by HS regime, based on kinetic equilibrium of the table with squeeze film effect consideration was proposed by Wang et al. [23], who found out that with increasing speed the error is more significant, but can be compensated with higher lubricant supply. Rajput and Sharma [24] investigated different geometric imperfections of

defined shapes and misalignment of journal bearing lubricated with HS regime using FEM formulation. All imperfections caused observably lower minimal film thickness, while the minimal film thickness was as twice as much lower in all cases with journal misalignment. As later observed by Zoupas et al. [25] using CFD analysis, different manufacturing error types (convex, concave, sine wave) have similar effects on the HD thrust bearings, as it was in the case of journal bearings. A new design of adjustable HS bearing with improved precision was proposed by Fedorynenko et al. [26]. Zhang et al. [27] presented a model based on formulations describing the relationship between geometric errors and motion errors in bearings lubricated with HS regime with an experimental validation. Zha et al. [28] later proposed tolerance design method for HS guideways based on error averaging effect, considering geometric parameters of guide rails with experimental validation.

The previous published available research provided insight into manufacturing error modelling and the use of compliant members. Nonetheless, an experimentally validated approach for investigation of compliant support applicability, and estimation of allowable assembly errors is missing.

Bearing efficiency

Unlike in case of small HSB, the power economy becomes a serious issue. The power consumption of HSB increases with the size. Therefore, it is crucial to optimize the bearing performance to reduce the operational costs. The calculation of a HSB performance and characteristics can be derived from N-S equations considering simplifications that lead to Reynolds equation for pressure distribution calculation. Based on the derived equations, analytical solutions for simple geometries, such as single recess rectangular or circular pad, were derived. In case of more complicated pad geometries, such as multi-recess pads, it is merely impossible, or extremely difficult to obtain analytical formulation. Therefore, experimental approach was used to obtain performance factors for a variety of pad proportions [29,30] based on electric analogy. This classical simplistic, yet effective approach has been used for decades to determine the pad geometry [31]. Nonetheless, with the advances in computational fluid dynamics, numerical modelling approach allowed to improve the design process of any bearing shape, while allowing to investigate flow characteristics and parameters that are difficult or even impossible to be measured experimentally. This approach has been increasingly applied on HS lubrication modelling [1]. It was successfully used for comparison of recess shapes by Yadav and Sharma [32] using FEM formulations. Helene et al. [8] used full Navier-Stokes equations in 2D geometry with structured mesh, including modelling turbulence effects to determine an optimal recess depth of HS journal bearings.

As shown in the provided state-of-the-art summary, many works aimed at numerical investigation of various recess shapes [33–37], but none of the available published research focused on assessing HSB performance by varying recess size and position of multi-recess HSB pad independently.

4 AIMS OF THE THESIS

The main aim of this PhD thesis is to introduce performance and safety improvements to the large-scale hydrostatic bearing design methodology. The thesis is focused on experimental and numerical analysis of hydrostatic bearing performance for different pad geometries and under bearing misalignment conditions. To achieve the main goal of this thesis, the necessary sub-aims are as follows:

- development and design of the experimental device,
- design of the methodology of experiments,
- design of data processing and evaluating,
- development of the methodology for pad shape optimization,
- series of experiments focused on the analysis of the bearing performance for the investigated cases and conditions,
- data analysis,
- discussion and publication of obtained results.

4.1 SCIENTIFIC QUESTIONS & HYPOTHESES

SQ1: What is the influence of HSB recess position and size on the bearing performance?

- **H1:** *Recess size and layout optimization based on separating geometric parameters can lead to improved pad performance and lower energetic losses.*

SQ2: How is the HS lubricating film affected by assembly errors of the bearing bodies?

- **H2:** *Pad misalignment can significantly affect the generation and uniformity of the HS lubricating film, which can compensate certain magnitude of pad misalignment. A compliant support can compensate larger misalignment compared to rigid support, while still ensure required performance.*
- **H3:** *Assembly errors of a segmented slider can lead to HS lubricating film non-uniformity and disruption. The maximal allowed error of the segmented sliders must be smaller than the film thickness to secure safe operation of the bearing.*

4.2 THESIS LAYOUT

The PhD thesis is composed of three original research papers published in peer-reviewed journals with impact factor. The content of the thesis is reflecting the scientific questions as stated above. Two main parts of the conducted research were determined: bearing efficiency and bearing safety, respectively, which are are further described in publications [I-III] in detail.

Bearing efficiency is linked with pad shape and the focus is aimed at pad geometry optimization, to reduce the power losses and thus energy consumption of the hydraulic pump. The first article [I] is focused on introducing a new two-parameter pad geometry optimization

method based on CFD simulation. The second part is dealing with bearing safety, specifically pad and slider misalignment effect on the bearing performance. The second article [II] is focused on investigation of pad misalignment effect on the bearing performance, and the effects of compliant support on misalignment compensation. The last article [III] is focused on assessing assembly errors of segmented sliders in stationary and low-speed conditions.

I.   MICHALEC, M., M. ONDRA, M. SVOBODA, J. CHMELÍK, P. ZEMAN, P. SVOBODA, R. L. JACKSON. A novel geometry optimization approach for multi-recess hydrostatic bearing pad operating in static and low-speed conditions using CFD simulation. Tribology letters, 2023, vol. 71, no. 2, p. 52. doi:10.1007/s11249-023-01726-3 [IF = 3.2] (Author's contribution 65 %)

II. MICHALEC, M., V. POLNICKÝ, J. FOLTÝN, P. SVOBODA, P. ŠPERKA, J. HURNÍK. 2022. The prediction of large-scale hydrostatic bearing pad misalignment error and its compensation using compliant support. Precision engineering, 2022, vol. 75, pp.67-79. doi:10.1016/j.precisioneng.2022.01.011 [IF = 3.6] (Author's contribution 40 %)

III. MICHALEC, M., J. FOLTÝN, T. DRYML, L. SNOPEK, D. JAVORSKÝ, M. ČUPR, P. SVOBODA. Assembly error tolerance estimation for large-scale hydrostatic bearing segmented sliders under static and low-speed conditions. Machines. MDPI, 2023, vol. 11, p.14. doi:10.3390/machines11111025 [IF = 2.6] (Author's contribution 54 %)

5 MATERIALS AND METHODS

The performed literature review led to outlining the knowledge gap in large-scale HSB. Based on the knowledge gap, scientific questions and hypotheses were formed. To investigate the scientific questions and hypotheses outlined in the previous chapters, experimental and numerical methods are employed in the presented study. The experimental and CFD simulation results were compared with analytical calculations to determine the precision of the measured and computed values, respectively. A schematical representation of the performed activities are shown in Figure 5. The employed experimental and numerical methods, methodology and experiment design are described in the following chapters in detail.
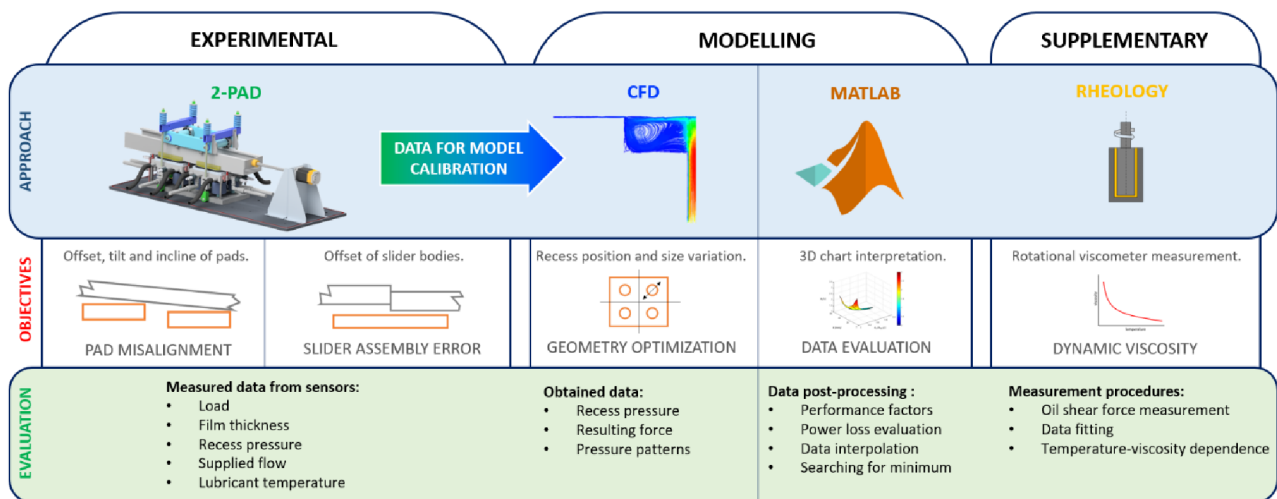

Figure 5 Schematical representation of the performed activities within the thesis.

5.1 Experimental devices

The experimental investigation was carried out on Dual-Pad Experimental HSB (2-PAD). To obtain inputs for the analytical calculation and CFD simulations, lubricant dynamic viscosity was measured using rotational viscometer.

5.1.1 Experimental hydrostatic bearing

The 2-PAD experimental device was designed at Institute of Machine and Industrial Design and introduced into function in 2020. 2-PAD consists of a loading frame that generates load on the slider, two HS pads mounted on pad supports with inlet channels. The slider can perform reciprocating motion driven by the electromotor.
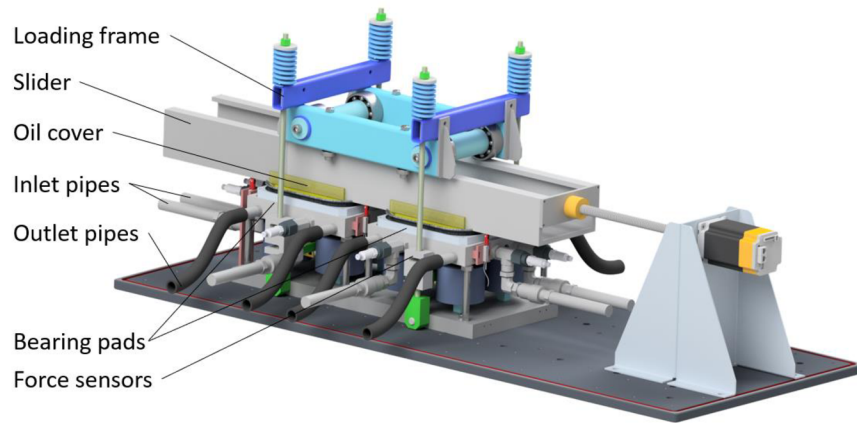
Figure 6 2-PAD experimental setup overview and laboratory view.

The experimental device was equipped with sensors (Figure 7) that allowed performing full online diagnostics of the bearing performance via controlling software build in the LabView environment. Proximity sensors mounted on pad supports provided direct measurement of the film thickness – six contactless sensors of 0.01 mm resolution. Four force sensors of range 10 kN and 2.5 N resolution allowed direct measurement of the applied load generated using threaded rods and compression springs. Temperature sensors built in the recess were used to evaluate actual dynamic viscosity based on the viscosity-temperature dependence. Pressure sensors of 160 bar range were used for obtaining information about the pressure in the recesses. The pad supports of 2-PAD were mounted on settings screws for the pad alignment based. For investigation of the compliant support, pads could be mounted on silentblocks with threaded ends instead.
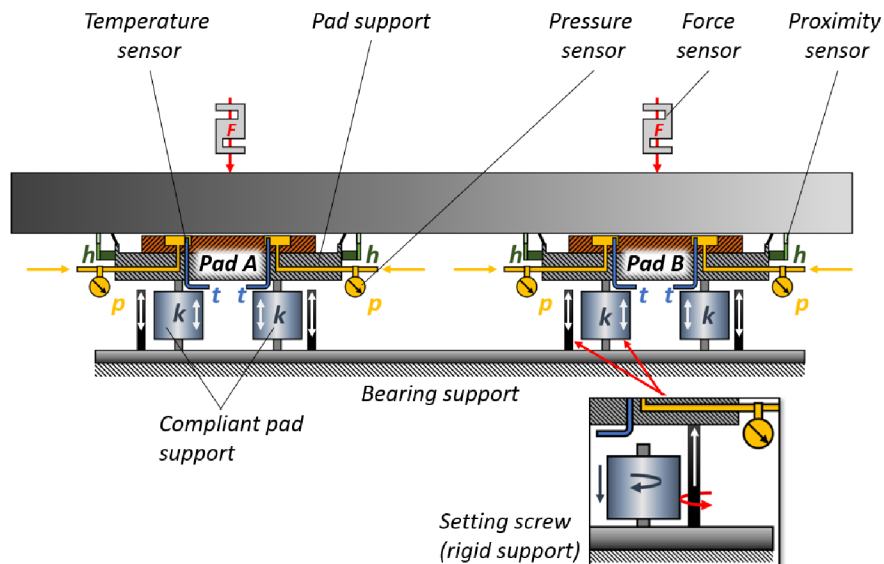

Figure 7 2-PAD sensor description and support type customization procedure.

The second, equally important part of the 2-PAD tester was the hydraulic circuit (Figure 8), which secures constant supply of the pressurized lubricant into the contact area and

maintains lubricating film separating the sliding surfaces of slider and pad. The hydraulic circuit was designed as single-pump, thus restrictors had to be assumed to evenly distribute the supplied flow of the lubricant into the recesses. The hydraulic circuit was equipped with safety components, such as pressure relief valve, check valves. The supplied flow and supplied pressure information were displayed on the motor controller and logged via the LabView control program. The selected lubricant for the experimental device was ISO VG 46 grade oil.
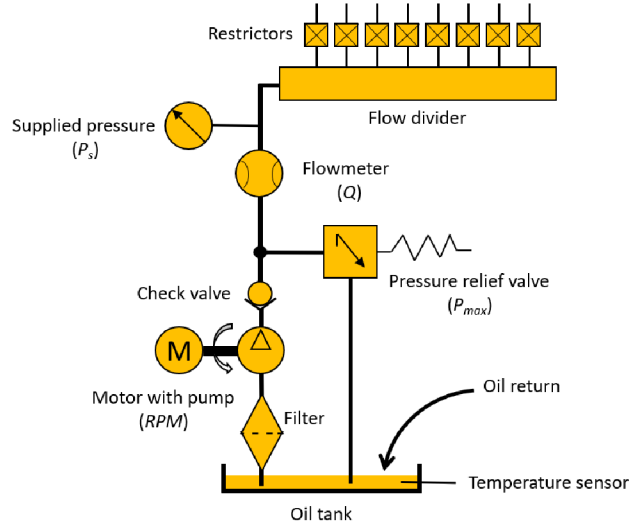

Figure 8 Hydraulic circuit scheme of the 2-PAD.

5.1.2 Viscometer

Dynamic viscosity is one of the primary variables that influence the bearing performance (Equation 1). Rotational viscosimeter HAAKE RotoVisco® 1 (PSL Systemtechnik, Germany) was used to obtain the lubricant dynamic viscosity dependency on temperature, thus actual viscosity could be evaluated in correspondence with the actual measured temperature in the recess region. The measured temperature was in range of 20 – 50 °C. The obtained coefficient for dependence were fitted using Vogel-Fulcher equation with R^2 = 99.87%. Final equation for dynamic viscosity evaluation was as follows:

$$\mu = 3.91 \cdot 10^{-5} \cdot e^{\left(\frac{1221}{T+131.5}\right)} \tag{1}$$

where T is lubricant temperature.

5.2 Numerical approach

Computational Fluid Dynamics (CFD) is a widely used method for analysis of fluid behaviour. Numerical analyses were performed using commercial software ANSYS Fluent 2021 R2 based on Finite Volume Method with Cell-Centered formulation. The calculation process could be divided into three main parts, as seen in Figure 9: pre-processing, solving and post-processing. Within the pre-processing stage, the 3D geometry was generated and transferred to discretization module Fluent Meshing. Subsequently, boundary conditions were set according to the experimentally obtained and measured data. Using the inputs, the case was solved until

reached desired residual magnitude, and then the calculated case was used for results evaluation and flow analysis.
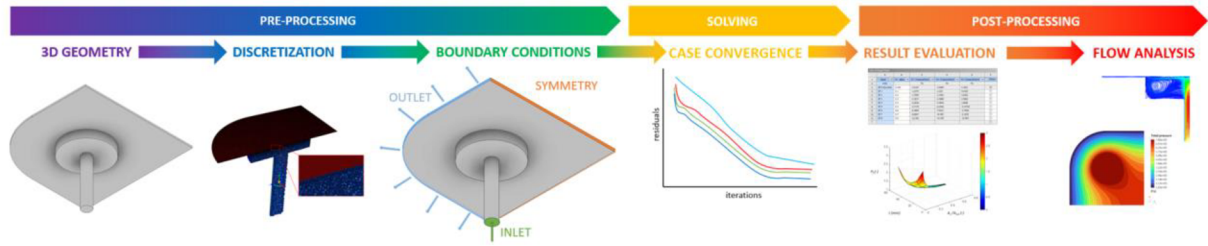

Figure 9 Schematical representation of the CFD solving processes.

After solving all parametrized design points in ANSYS Fluent, the data obtained from simulations were transferred to MATLAB for further evaluation. As seen in Figure 10, the classical 1-parameter optimization approach uses only one variable parameter, recess size a, or recess position/pad size t. The proposed 2-parameter approach works with two geometric parameters, recess position p and recess-to-pad size ratio A_r/A_{tot}, independently. The programmed MATLAB script generated 3D charts for each of the performance factors independently and then created the power loss factor interpolated surface, which was discretized into smaller areas to obtain more precise coordinates for minimal power loss factor H_f. Subsequently, using the coordinates, an optimized pad geometry could be created.
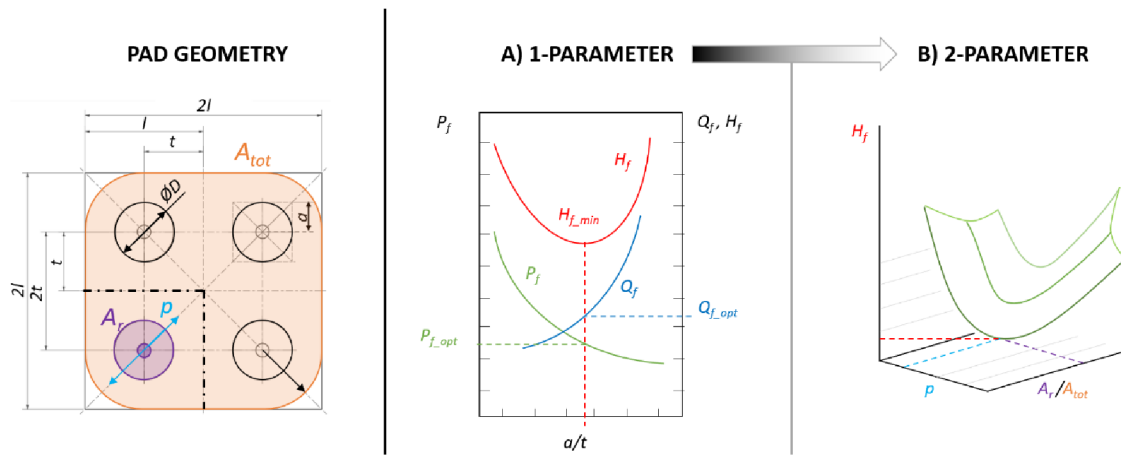

Figure 10 Schematical representation of A) classical 1-parameter approach and B) novel 2-parameter approach geometry optimization.

5.3 Methodology and experiment design

The methods used for the investigation of defined scientific questions and hypotheses were analytical, numerical, and experimental. Firstly, the analytical formulation was employed to verify the results obtained from the remaining two approaches. The thesis investigation was divided into two main areas, namely bearing efficiency, and bearing safety, respectively. Those areas are described in the following chapters in detail.

5.3.1 Bearing efficiency

The classical approach to HSB pad recess layout and size optimization is based on finding the minimal value of power loss factor, what is represented by an optimal ratio for the highest load capacity at lowest supplied flow. Then, an optimal ratio between recess radius and recess position (a/l) is determined. In case of pad geometry as shown in *Figure 10*, an optimal a/l ratio is 0.4. Subsequently, the geometry is adjusted according to the obtained ratio. Nonetheless, the described classical approach constrains the two geometrical parameters – recess size and recess position, together. Therefore, a numerical study was performed to investigate the bearing performance of the two geometric parameters, recess size and position, independently. In this approach, all three approaches (analytical, experimental, and numerical) were combined to validate the numerical model result precision. The methodology steps were divided into four main parts: numerical model establishment, domain discretization, numerical model calibration and results evaluation. Firstly, a parametric 3D model was established for an automated geometry customization after each finished case calculation. To reduce the computational time and improve model precision, one-quarter model was created and discretized using symmetry regions and assessed based on Richardson Extrapolation method. The boundary conditions were set according to the experimentally obtained results and the calculation was performed. Finally, the results for recess pressure, pressure contours and resulting force on the top plane were evaluated and discussed.

5.3.2 Bearing safety

The investigation of assembly errors was divided into two main branches – pad misalignment and slider segment misalignment, respectively. For those cases, only analytical and experimental methods were employed. The bearing performance and behaviour was judged based on experimental data, while the analytical approach served to check the generated data validity.

A) Pad misalignment

The investigation of maximal allowable misalignment errors of HSB pads was performed completely under static conditions. The first step was to identify the misalignment types that can occur during the assembly (*Figure 11*). Nonetheless, the misalignment had to be within the range of proximity sensors (0 – 3 mm). The misalignment errors were set using SKF calibrated shims. All pad misalignment types were measured for a range of error magnitudes with rigid support. Subsequently, a compliant support consisting of three silentblocks sets of different stiffness were measured. The stiffnesses were chosen according to the expected loads and the error compensation range.
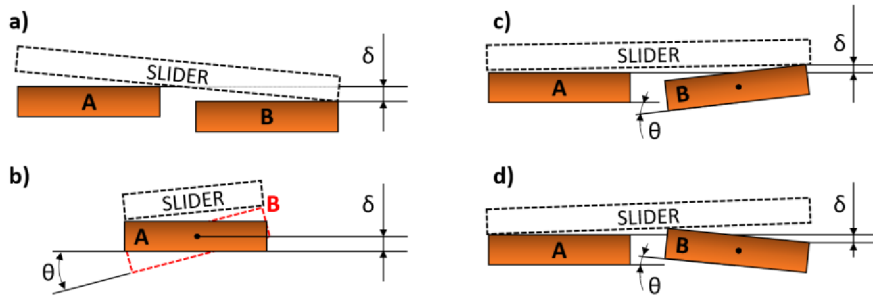
Figure 11 Pad misalignment error types: a) offset, b) inclination, c) tilt 1 and d) tilt 2.

B) Slider segment misalignment

The estimation of slider segment assembly error tolerance was carried out on the 2-PAD tester with a slider consisting of two parts with a bolted connection. The error was generated in the connection using SKF calibrated shims for two cases – offset and tilt, respectively (Figure 12). The error magnitudes were used in the error-to-film thickness ratio (e/h) for better transferability of obtained results for different scales. The "step-up" and "step-down" offset error types were investigated to determine the offset error type and critical error value for both directions of the slider movement.
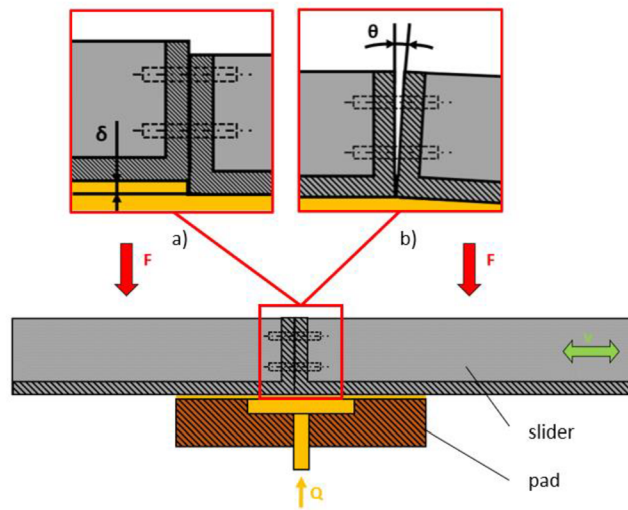

Figure 12 2-PAD Segmented slider error types a) offset and b) tilt.

6 RESULTS AND DISCUSSION

The experimental investigation was conducted on the 2PAD device. As indicated in the materials and methods section, the focus was aimed at two main goals – performance improvement with special attention laid on geometry optimization and safety improvements with special attention laid on assembly errors of segmented sliders and pads.

6.1 Geometry optimization

The geometry optimization based on parametric study carried out using CFD resulted in 3D graphs for performance factor, flow factor and by combination of the two factor, performance factor was obtained. The 3D graphs, in comparison with the classical approach by Rippel [104] uses independent variation of recess position and size.

To determine the optimal shape of the bearing, the minimum power loss factor was searched for. To obtain a more accurate result, the minimum was not chosen from the calculated values of the design points, but by using a cubic interpolated surface as seen in Figure 13. This step allowed us to look for the minimum value of the power loss factor also between the calculated points. The calculated points were used to fit the cubic interpolated surface with normalization in MATLAB R2021a. It is also possible to use linear interpolation, which is simpler but does not capture the surface trend and curvature as well as the cubic interpolation. Subsequently, a minimum value of the power loss factor was found. Then, the coordinates of the minimum value expressed the optimal shape – the recess position and area ratio, respectively. The minimum value of the power loss factor, 30.66, obtained by CFD simulation was determined for the recess position 17.66 mm from the centre and an area ratio of 0.2. In contrast, optimal value of the power loss factor obtained from the graph presented by Loeb and Rippel [105] is 38, with recess position of 35 mm and area ratio of 0.132. Compared to the basic approach using one-parameter criteria, a 20 % reduction of the power loss factor was achieved. The investigated ranges of recess position and area ratio were chosen according to the pad size and computable geometry. The interpolated grid could be finer if even higher precision was required.
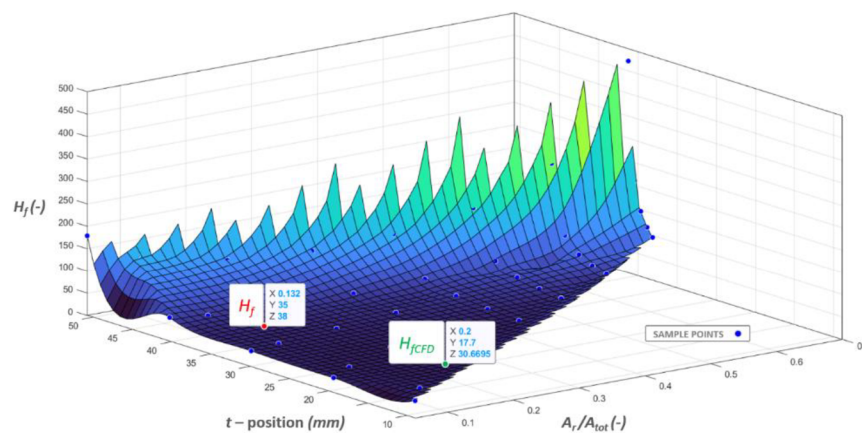

Figure 13 Power loss factor cubic interpolation of results obtained from CFD analysis with highlighted minimal power loss factor for 2-parameter optimization (H_{fCFD}) and using 1-parameter optimization (H_f) based on [105].

Finally, we compared the pressure contours of the optimal shape obtained from the classical approach (Figure 14 a) and the presented two-parameter approach (Figure 14 b), respectively. The classical approach optimization resulted in smaller recess diameter and its farther position from the pad centre compared to the two-parameter approach, which also resulted in higher recess pressure due to larger sealing edge. As can be seen in the comparison of the two pressure contours (Figure 14), the one-parameter approach performed with pressure decrease in the central area, while the two-parameter approach showed uniform pressure among the four recesses. The results indicate that the proposed method provides more uniform pressure distribution and contributes to higher bearing load capacity, stiffness, and ability to carry asymmetrical loading and pad misalignment. The only drawback of this geometry might be worsened ability to assess the behaviour of each of the recesses separately. Nonetheless, discharge grooves can be added to solve this issue [26].
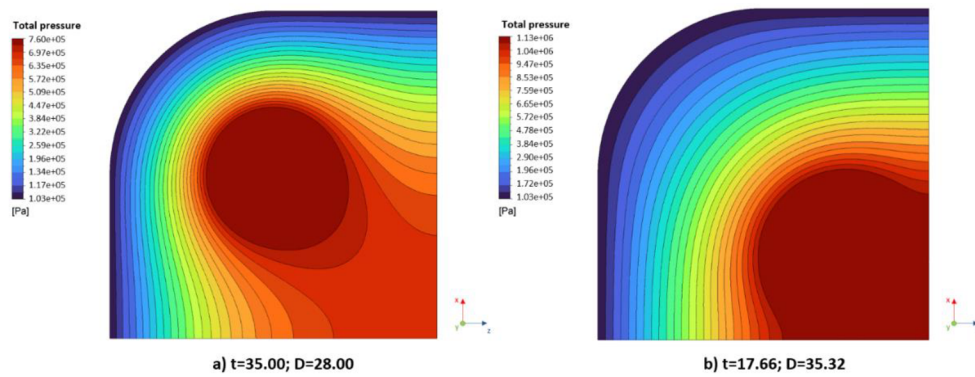

a) t=35.00; D=28.00   b) t=17.66; D=35.32

Figure 14 Top plane static pressure contours of optimized pad shapes using a) one-parameter approach and b) novel two-parameter approach.

6.2 Pad misalignment

The comparison of investigated misalignment types is shown in *Figure 15*. To express the significance of the compliant support effect, the relative change of recess pressure to the initial recess pressure (with aligned sliding surfaces) was used as an evaluation criterion. Firstly, the difference was calculated for each sensor. Then the obtained values were divided by the initial film thickness, and then an average value was calculated. As shown in *Figure 15* a, the compliant pads adjusted to the occurred assembly error and caused a more even distribution of the pressurized fluid for at least twice in case of the TILT 2 error type, five times and eight times in case of the OFFSET and INCLINE errors respectively. TILT 1 did not show any significant difference with compliant pads in the recess pressure, which might be caused by a greater space for the slider deformation. A similar trend was observed with the film thickness relative change (*Figure 15* b). The INCLINE error type resulted in three times, TILT 2 3.8 times, TILT 1 twice, and the OFFSET 5.3 times smaller relative film thickness change with medium compliant pads. The results clearly indicate that the compliant pads create more evenly distributed film thickness and pressure.
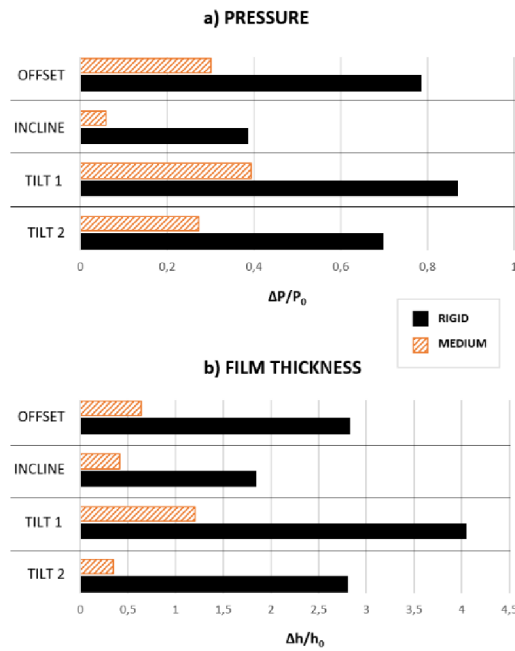
Figure 15 Relative change of a) pressure and b) film thickness of rigid and compliant support (medium stiffness) for all studied misalignment types with 0.5 mm misalignment and 16 kN load.

The obtained results show that the compliant support could provide a uniform film thickness along the slider and evenly distributed pressure in the recesses. To show the oil pressure distribution and film thickness, we selected only one misalignment type – OFFSET, which is probably the most problematic error from the presented ones because it is necessary to be set to all pads to achieve as high as possible sliding surface flatness. The obtained recess pressure values are shown in *Figure 16* for a) rigid support and b) compliant support with compliant pads of medium stiffness with the outlined average pressure values from *Figure 16*. The rigidly supported hydrostatic bearing showed slightly higher local pressures (12 bar) compared to the compliant supported hydrostatic bearing (9.2 bar). However, the rigid support shows significantly greater differences in the recess pressure among all recesses, while the compliant support evidently distributes the lubricant pressure more evenly. The difference between the predicted and experimental values is most probably caused by a local increase and decrease in the lubricating film stiffness local according to the misalignment magnitude and slider position relative to the bearing pads. The local pressure decrease possibly causes the lubricating film stiffness to decrease and vice versa. Therefore, the load-carrying ability for certain misalignment types is higher than in the prediction.
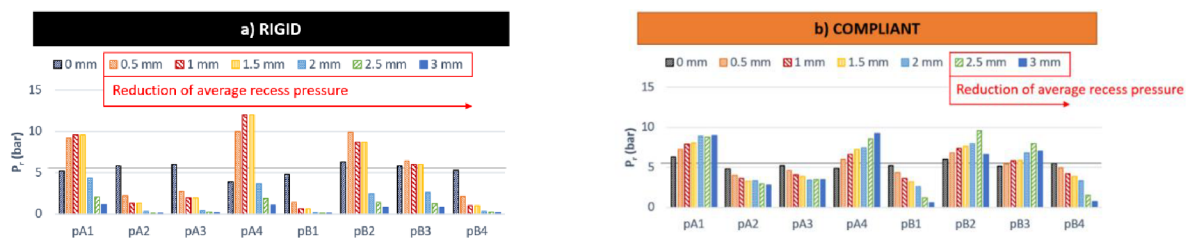

Figure 16 Recess pressure values of OFFSET measurements for height difference δ (0, 0.5, 1, 1.5, 2, 2.5, and 3 mm) with a) RIGID and b) COMPLIANT (medium stiffness) support.

The results support the assumption that the compliant support significantly reduces the differences in the film thickness compared to the rigid support. The results show that a more than 50 % smaller change of the film thickness was achieved using the compliant support. Therefore, the sensitivity to the misalignment error is greatly lower with the use of a compliant support for the hydrostatic bearing pads. The experimental results of film thickness indicate that the lubricating film stiffness is not constant along the slider in a misaligned bearing. Therefore, the maximum assembly error is actually higher than the predicted one as shown in *Figure 17*, which emphasises the significance of the restrictor use in the hydrostatic bearing systems.
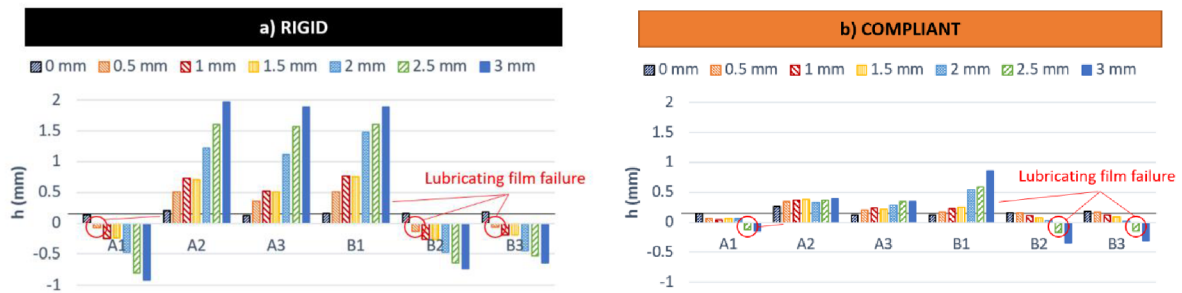

Figure 17 Film thickness values of OFFSET measurements for height difference δ (0, 0.5, 1, 1.5, 2, 2.5, and 3 mm) with a) RIGID and b) COMPLIANT (medium stiffness) support.

The compliant pad stiffness effect on the performance of the hydrostatic bearing with misaligned surfaces was investigated only for the OFFSET error. The recess pressure and film thickness relative change (Δp and Δh) with misaligned pads divided by the initial values (p_0 and h_0) obtained for levelled pads was used as the evaluation criteria. Hence, the relative change of the a) recess pressure and b) film thickness is shown in *Figure 18*. It is evident that the hydrostatic bearing rigid support does not allow for even distribution of the pressure and uniform film thickness along the slider. The relative change of the film thickness is greater with increasing offset misalignment for all support types. In comparison with the rigid support, for the 3 mm offset a significant 56 % reduction in recess pressure, and a 70 % decrease in film thickness relative change were achieved using soft compliant pads. Therefore, it is evident that the lower support stiffness, the better the ability to adjust the pads' sliding surfaces to the slider. Thus, the bearing performance with compliant support shows significantly better performance and much lower sensitivity to the assembly errors. However, we want to emphasize that the use of compliant support for error compensation can only be used in applications that do not require high bearing stiffness, such as machining centres, precision guideways, or optical telescopes. On the contrary, it might be highly desirable in large-scale low-precision applications to reduce costs related to the manufacturing, assembly, and service.
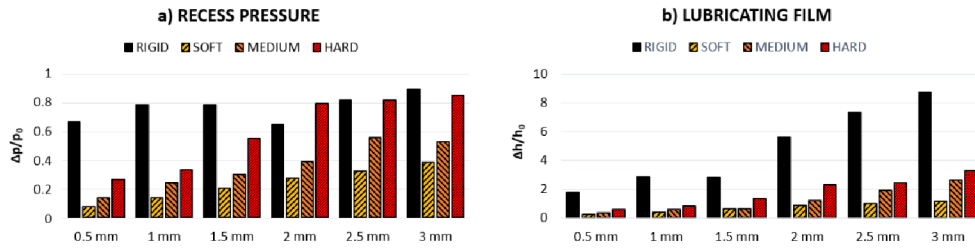
Figure 18 Compliant support stiffness comparison of the relative change to the initial value of a) recess pressure and b) lubricating film.

6.3 Segmented slider misalignment

The tilt assembly error type was assessed for two positions – "mid-pad" (*Figure 19* A) and "mid-bearing" (*Figure 19* B) configurations. The judging criteria were the average pressure of both pads, pressure in all recesses, film thickness obtained from proximity sensors, and initial film thickness 0.13 mm at $\theta = 0$. The normal pressure for the supplied flow and load was again 0.68 MPa. The bearing performed normal operation within the angular error $\theta = 0 - 0.4$ °. In the case of the "mid-pad", the average recess pressure slowly decreased, starting at $\theta = 0.2$ ° until $\theta = 0.42$ °. The range of $\theta = 0.46 - 0.5$ ° was considered as the critical error range for the "mid-pad" error type. The limiting value that would allow the bearing to be functional was 0.5 °. Regarding the "mid-bearing" error type, the average recess pressure was relatively stable until the tilt angular error reached a value of $\theta = 0.75$ °. Any further added error caused the average recess pressure to rapidly decrease. Due to the rapid decrease in the average recess pressure with increased error value, the critical error range is relatively small, within $\theta = 0.78 - 0.8$ °. Any error greater than $\theta = 0.8$ ° would mean a loss of the load carrying ability. However, a relative movement of the pad and slider bodies is required for proper bearing function. Therefore, the angular error of $\theta = 0.46$ ° is considered the limit value for which the bearings can operate normally under static conditions in the two investigated positions. Considering that the slider will move during operation, the "mid-pad" error type allows a smaller error tolerance. The highest value of θ is 0.5 °. Any higher error would lead to a contact of solid bodies for the tilt error type. The pads were positioned at ratio of pad centre distance to pad edge length of 2.3. Nonetheless, if the distance of the pads was greater, the angular tolerance would decrease.
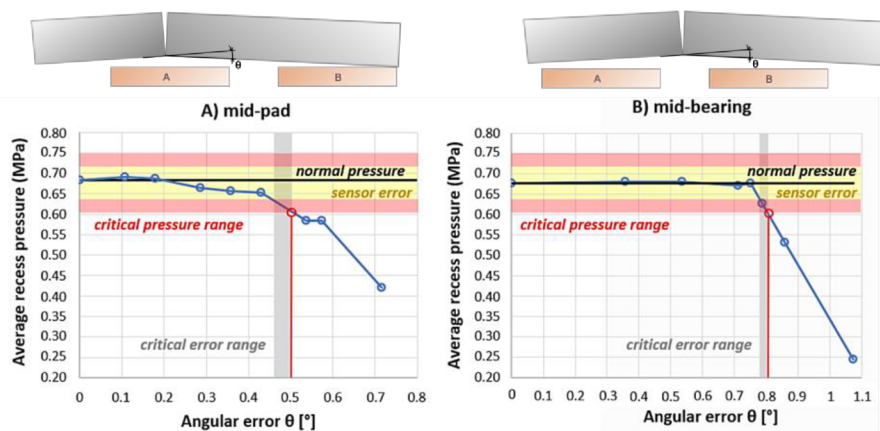

Figure 19 Average recess pressure dependency on angular error (tilt) of the slider bodies for cases A) in the middle of pad A and b) in between the pads A & B.

The "step-up" (Figure 11) dynamic tests were performed for a range of errors (e) from 0.05 – 0.3 mm with 0.05 increment. The average recess pressure trend was very similar for all cases, therefore, only runs of 0.1 mm, 0.2 mm, and 0.3 mm errors (e) are drawn in Figure 20. The measured data show an almost identical rise of the average recess pressure when the edge passes through the pad land area (between points I. and II.). This is caused by decreasing the effective area of pad A while carrying the same load, thus the pressure increases. However, as soon as the slider step approaches the recess area (point II.), the pressure rapidly decreases, depending on the magnitude of the error. If the error (e) was within 0.05 – 0.015 mm, the pressure was still within the sensor error area and did not reach the critical pressure range. However, the pressure with a 0.2 mm error (equivalent to the ratio e/h = 1.5) has already entered the critical pressure range and is considered as the limiting value of error for the investigated movement speed. After the edge passed the recess area, the average pressure stabilized at higher value in case of smaller errors (e < 0.2 mm). The errors within the range of 0.2 – 0.3 mm (e/h = 1.5 – 2.3) exhibited average pressures below the critical pressure range. This is also a matter of the restrictor setup and their performance. The test was terminated when the edge reached middle of the pad A (point IV.).
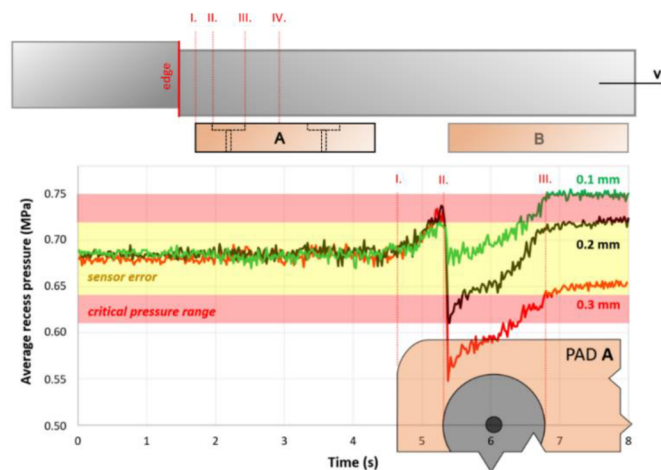
Figure 20 Average recess pressure value evolution in time for "step-up" error at 38 mm/s movement speed.

The "step-down" dynamic tests were performed for a range of errors (e) of 0.05 – 0.3 mm with 0.05 mm increment. In the error range (e) of 0.05 – 0.15 mm (e/h = 0.38 – 1.15), the bearing could operate normally and did not exhibit any form of collision. As seen in *Figure 22*, the assumed 0.15 mm error was smaller, approximately 0.1 mm instead of 0.15 mm. Moreover, the average recess pressure, as seen in *Figure 22* was slightly higher than the critical pressure after passing the recess area (starting with point III.), it did not fall below the lower critical value, thus we assumed normal operation. The tests were terminated when the edge reached middle of the pad A (point IV.). An actual problem with the bearing performance started to arise at 0.2 mm error (e/h = 1.54), whose real value seems to be, according to the obtained data from sensors 0.15 mm.
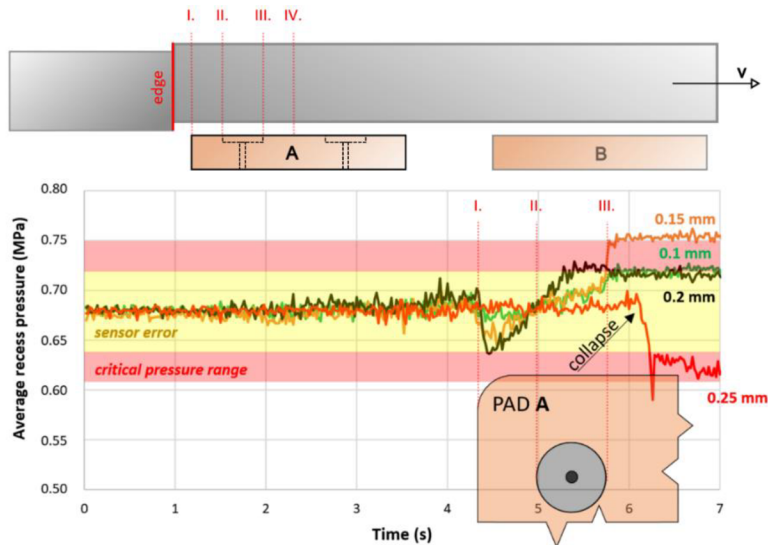
Figure 21 Average recess pressure value evolution in time for "step-down" error at 38 mm/s movement speed.

As seen in Figure 21, the "0.2 mm" error exhibited rapid decrease of the average pressure when the edge entered the pad area (point I.), but the bearing was able to react to the change with increased pressure. This type of error was not as sensitive to the average recess pressure (between points II. and III.) as the "step-up" type but was more dangerous from the film thickness point of view. The bearing pad could not handle such error at higher speeds. As expected, this type of offset error was more dangerous, and the slider and pad collision occurred at 0.25 mm error (e/h = 1.92). The motor managed to pull the slider despite contact was observed (the slider stopped for a while and then moved further). Therefore, the "step-down" tolerance must be within the film thickness height, thus the ratio e/h should be smaller than 1 to avoid collision of the solid bodies. Although the average recess pressure almost did not reach the critical pressure area, the film thickness (Figure 22) was already around zero, which means that the slider error edge and pad were almost at the same level.

Figure 22 Film thickness evolution in time for the "step-down" error at 38 mm/s movement speed.

7 CONCLUSIONS

The dissertation thesis deals with large-scale HSB performance and safety improvement. The attention of research teams all over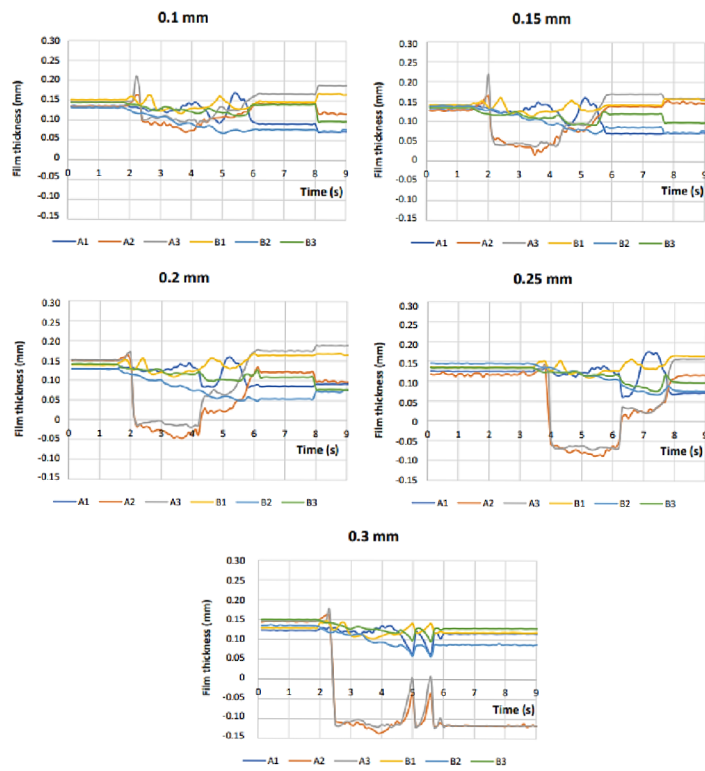 the world is mainly drawn by performance optimization and geometric error effect investigation on precision and bearing performance. Even though the HS lubrication was firstly demonstrated in the 19th century, the research interest in this lubrication regime has been rising over the years and is still growing. Multiple approaches to design and optimization of such bearings were proposed over the years and a huge proportion of researchers and design engineers rely on them. Nonetheless, there are still some design aspects and procedures that are performed in an old-fashioned and not very effective way or performed by estimation without an experimentally or numerically supported results. One of the primary factors of HS lubrication is the bearing geometry. The classical experimentally derived optimization method based on single-parameter pad shape optimization seems to serve well as a first iteration in design process, but further customization of the pad geometry might reduce the energy losses of the pump. The manufacturing precision and motion errors have been described in much detail, what allowed to improve the precision of HSB. Another very important factor is the precision of the HSB solid bodies, especially the assembly precision in the case of large-scale bearings. Pad misalignment was studied very briefly, with little attention paid to compliant support investigation. Segmented slider assembly errors have not yet been studied, even though large-scale HSB sliders are not possible to be manufactured in desirable precision for diameters exceeding tens of metres.

The first part of the thesis discusses all aspects of large-scale HSB design and optimization, including performance analyses, errors, and materials. Subsequently, a novel approach to multi-recess pad geometry optimization using CFD is presented and validated based on experimental and analytical data. The latter part deals with pad and slider segment misalignment, based on experimental measurements.

The main aim of this thesis was to improve HSB performance and safety with the use of experimental and numerical methods. To be able to investigate the bearing performance in various cases and scenarios, an experimental HSB test rig was designed and developed as a part of the PhD thesis in collaboration with colleagues at the Institute of Machine and Industrial Design. The experimental rig data accuracy was validated against analytical data. Subsequently, methodological approach for geometry optimization using CFD simulation is presented and validated. Finally, allowed misalignment magnitudes of pad and slider segments are determined based on experimental data.

The presented thesis presents original results extending the knowledge in the area of hydrostatic bearing performance and safe operation. The results are confronted with previously published studies. The further step is to employ to develop a comprehensive methodology for large-scale bearings working in the HS regime under real variable conditions.

The main contribution of the thesis can be summarized into the following points:

- A comprehensive summary of previously published research, current trends and future scope aimed at large-scale HSB design and optimization approaches was performed.
- A novel multi-recess pad shape optimization method of HSB based on CFD was developed.
- Experimental-based methodology for HSB compliant support design was suggested and compared with rigid support.
- For the first time, assembly errors of segmented sliders were assessed and experimentally investigated under static and low-speed conditions.

Regarding to scientific questions from chapter 4.1, the obtained knowledge can be summarized to the following concluding remarks:

A) Bearing performance

SQ1: What is the influence of hydrostatic bearing recess position and size on the bearing performance?

H1: HYPOTHESIS WAS VERIFIED:

- *HSB pad geometry is one of the key parameters influencing its performance. The classical optimization approach is based on one parameter optimization of the recess size and position linked together. The proposed two parameter method shows that by adjusting recess size and position separately can influence the bearing performance and reduce energy losses up to 20 %.*

B) Bearing safety:

SQ2: How is the hydrostatic lubricating film affected by assembly errors of the bearing bodies?

H2: HYPOTHESIS WAS VERIFIED:

- *As the previous research indicated, compliant pad support for multi-pad HSB can help to compensate pad misalignment. Compared to the rigid support, compliant support allows 4 to 6 times larger misalignment depending on the misalignment type.*

H3: HYPOTHESIS WAS VERIFIED:

- *The segmented slider errors, inclination and offset, have larger error tolerance under static conditions, depending on the distance between pads of multi-pad HSB when compared to the film thickness. As investigated the offset error under slow-speed conditions, the maximal allowed error to avoid solid bodies collision must be smaller than the film thickness.*

REFERENCES

[1]   O. Reynolds, "On the Theory of Lubrication and Its Application to Mr. Lowe's Experiments," *Philos Trans R Soc Lond*, vol. 177, pp. 157–234, 1886.

[2]   Lord Rayleigh O.M. F.R.S., "Notes on the theory of lubrication," *The London, Edinburgh, and Dublin Philosophical Magazine and Journal of Science*, vol. 35, no. 205, pp. 1–12, 1918,

[3]   M. M. Khonsari *et al.*, *Applied Tribology: Bearing Design and Lubrication*, vol. 3, no. 2. Chichester, UK: John Wiley & Sons, Ltd, 2017.

[4]   W. B. Rowe, "Advances in hydrostatic and hybrid bearing technology," *Proc Inst Mech Eng C J Mech Eng Sci*, vol. 203, no. 4, pp. 225–242, 1989,

[5]   R. Bassani *et al.*, *Hydrostatic Lubrication*, 22nd ed. Elsevier B.V., 1992.

[6]   X. B. Li *et al.*, "The Research Status and Progress of Heavy/Large Hydrostatic Thrust Bearing," *Advances in Mechanical Engineering*, 2014,

[7]   Z. F. Liu *et al.*, "A review of hydrostatic bearing system: Researches and applications," *Advances in Mechanical Engineering*, vol. 9, no. 10, 2017,

[8]   R. Mahdi *et al.*, "Experimental investigations on stick-slip phenomenon and friction characteristics of linear guides," *Procedia Eng*, vol. 100, no. January, pp. 1023–1031, 2015,

[9]   J. Awrejcewicz *et al.*, "The Occurrence of Stick-Slip Phenomenon," no. June 2014, 2017.

[10]   A. BONANNO *et al.*, "a Study on the Structureborne Noise of Hydraulic Gear Pumps," *Proceedings of the JFPS International Symposium on Fluid Power*, vol. 2008, no. 7–3, pp. 641–646, 2008,

[11]   V. Induced *et al.*, "Vibrations Induced by Internal Fluid Flow," *Flow-induced Vibrations*, no. i, pp. 157–195, 2014,

[12]   H. Ortwig, "Experimental and analytical vibration analysis in fluid power systems," *Int J Solids Struct*, vol. 42, no. 21–22, pp. 5821–5830, 2005,

[13]   G. Chen *et al.*, "Load performance of large-scale rolling bearings with supporting structure in wind turbines," *J Tribol*, vol. 134, no. 4, 2012,

[14]   G. Chen *et al.*, "Effects of size and raceway hardness on the fatigue life of large rolling bearing," *Journal of Mechanical Science and Technology*, vol. 29, no. 9, pp. 3873–3883, 2015,

[15]   L. Chen *et al.*, "Rework solution method on large size radial roller bearings," *Journal of the Brazilian Society of Mechanical Sciences and Engineering*, vol. 38, no. 4, pp. 1249–1260, 2016,

[16]   R. Bassani, "Hydrostatic self-regulating multipad journal and integral bearings," *Tribology Transactions*, vol. 56, no. 2, pp. 187–195, 2013,

[17]   J. Y. Jang *et al.*, "On the characteristics of misaligned journal bearings," *Lubricants*, vol. 3, no. 1, pp. 27–53, 2015,

[18]   E. A. Novikov *et al.*, "Calculation of the characteristics of a hydrostatic ring thrust bearing for refrigeration compressors," *Chemical and Petroleum Engineering*, vol. 40, no. 3–4, pp. 222–228, 2004,

[19]   M. Sheehan *et al.*, "Progress on the structural and mechanical design of the Giant Magellan Telescope," *Ground-based and Airborne Telescopes IV*, vol. 8444, p. 84440N, 2012,

[20]   M. Johns *et al.*, "Design of the Giant Magellan Telescope," *Ground-based and Airborne Telescopes V*, vol. 9145, p. 91451F, 2014,

[21]   S.-H. Jang *et al.*, "Development of Core Technologies of Multi-tasking Machine Tools for Machining Highly Precision Large Parts," *Journal of the Korean Society of Precision Engineering*, vol. 29, no. 2, pp. 129–138, 2012,

[22]   Z. Guo *et al.*, "Application of CFD analysis for rotating machinery - Part I: Hydrodynamic, hydrostatic bearings and squeeze film damper," *J Eng Gas Turbine Power*, vol. 127, no. 2, pp. 445–451, 2005,

[23]   A. Bouzidane *et al.*, "Nonlinear Dynamic Analysis of a Rigid Rotor Supported by a Three-Pad Hydrostatic Squeeze Film Dampers," *Tribology Transactions*, vol. 56, no. 5, pp. 717–727, 2013,

[24]   Z. Liming *et al.*, "A review on the large tilting pad thrust bearings in the hydropower units," *Renewable and Sustainable Energy Reviews*, vol. 69, no. September 2016, pp. 1182–1198, 2017,

[25]   D. V. De Pellegrin *et al.*, "An isoviscous, isothermal model investigating the influence of hydrostatic recesses on a spring-supported tilting pad thrust bearing," *Tribol Int*, vol. 51, pp. 25–35, 2012,

[26]   M. Wasilczuk, "Friction and lubrication of large tilting-pad thrust bearings," *Lubricants*, vol. 3, no. 2, pp. 164–180, 2015,

[27]   X. Raud *et al.*, "Numerical modelling of hydrostatic lift pockets in hydrodynamic journal bearings – Application to low speed working conditions of highly loaded tilting pad journal bearings," *Mechanics and Industry*, vol. 14, no. 5, pp. 327–334, 2013,

[28]   R. A. J. Van Ostayen *et al.*, "A mathematical model of the hydro-support: An elasto-hydrostatic thrust bearing with mixed lubrication," *Tribol Int*, vol. 37, no. 8, pp. 607–616, 2004,

[29]   E. Xu *et al.*, "Investigations on the applicability of hydrostatic bearing technology in a rotary energy recovery device through CFD simulation and validating experiment," *Desalination*, vol. 383, pp. 60–67, 2016,

[30] Z. Liu *et al.*, "Design and manufacturing model of customized hydrostatic bearing system based on cloud and big data technology," *International Journal of Advanced Manufacturing Technology*, vol. 84, no. 1–4, pp. 261–273, 2016,

[31] I. F. Santos, "Controllable sliding bearings and controllable lubrication principles-an overview," *Lubricants*, vol. 6, no. 1, 2018,

[32] T. Seperamaniam *et al.*, "Hydrostatic Bearing Design Selection for Automotive Application Using Pugh Controlled Convergence Method," *Procedia Eng*, vol. 170, pp. 422–429, 2017,

[33] A. Harnoy, *Bearing design in machinery, Engineering tribology and lubrication*. 2003.

[34] K. Cheng *et al.*, "A selection strategy for the design of externally pressurized journal bearings," *Tribol Int*, vol. 28, no. 7, pp. 465–474, 1995,

[35] M. Kozdera *et al.*, "Numerical modelling of the flow in the annular multi-recess hydrostatic thrust bearing using CFD methods," *EPJ Web Conf*, vol. 45, 2013,

[36] M. Sheehan *et al.*, "Progress on the structural and mechanical design of the Giant Magellan Telescope," *Ground-based and Airborne Telescopes IV*, vol. 8444, p. 84440N, 2012,

[37] S.-H. Jang *et al.*, "Development of Core Technologies of Multi-tasking Machine Tools for Machining Highly Precision Large Parts," *Journal of the Korean Society of Precision Engineering*, vol. 29, no. 2, pp. 129–138, 2012,

[38] B. M. A. Maher, "Performance characteristics of an elliptic hydrostatic bearing and comparative analysis based on Stokes' conditions," *Acta Mech*, vol. 223, no. 6, pp. 1187–1198, 2012,

[39] B. J. Hamrock *et al.*, *Fundamentals of Fluid Film Lubrication*, 2nd ed. New York : Marcel Dekker, 2004.

[40] H. C. Rippel, "Cast bronze bearing design manual," 1960.

[41] D. Chen *et al.*, "Performance evaluation and comparative analysis of hydrostatic spindle affect by the oil film slip," *J Manuf Process*, vol. 20, pp. 128–136, 2015,

[42] S. Gao *et al.*, "CFD based investigation on influence of orifice chamber shapes for the design of aerostatic thrust bearings at ultra-high speed spindles," *Tribology International*, vol. 92. pp. 211–221, 2015.

[43] F. Ghezali *et al.*, "3D Numerical investigation of pressure field of an orifice compensated hydrostatic bearing," *Mechanics & Industry*, vol. 18, no. 1, 2017,

[44] F. Shen *et al.*, "Effect of Pocket Geometry on the Performance of a Circular Thrust Pad Hydrostatic Bearing in Machine Tools," *Tribology Transactions*, vol. 57, no. 4, pp. 700–714, 2014,

[45] S. Yang *et al.*, "A study of inlet temperature models of a large size tilting thrust bearing comparison between theory and experiment," *Tribol Int*, vol. 140, no. March, p. 105881, 2019,

[46] X. Li *et al.*, "The research status and progress of heavy/large hydrostatic thrust bearing," *Advances in Mechanical Engineering*, vol. 2014, 2014,

[47] D. Fedorynenko *et al.*, "Dynamic characteristics of spindle with water-lubricated hydrostatic bearings for ultra-precision machine tools," *Precis Eng*, vol. 63, no. January, pp. 187–196, 2020,

[48] Y. T. Zhang *et al.*, "Error Averaging Effect of Hydrostatic Journal Bearings Considering the Influences of Shaft Rotating Speed and External Load," *Ieee Access*, vol. 7, pp. 106346–106358, 2019,

[49] J. Zha *et al.*, "Straightness error modeling and compensation for gantry type open hydrostatic guideways in grinding machine," *Int J Mach Tools Manuf*, vol. 112, no. August 2016, pp. 1–6, 2017,

[50] F. Xue *et al.*, "Research on error averaging effect of hydrostatic guideways," *Precis Eng*, vol. 36, no. 1, pp. 84–90, 2012,

[51] H. Zhang *et al.*, "Optimization of texture shape based on Genetic Algorithm under unidirectional sliding," *Tribol Int*, vol. 115, pp. 222–232, 2017,

[52] E. Solmaz *et al.*, "Multicriteria optimization approach for hydrostatic bearing design," *Industrial Lubrication and Tribology*, vol. 54, no. 1, pp. 20–25, 2002,

[53] D. Fedorynenko *et al.*, "Accuracy of spindle units with hydrostatic bearings," *Acta Mechanica et Automatica*, vol. 10, no. 2, pp. 117–124, 2016,

[54] D. Fedorynenko *et al.*, "Increasing of energy efficiency of spindles with fluid bearings," *Acta Mechanica et Automatica*, vol. 11, no. 3, pp. 204–209, 2017,

[55] Y. Wang *et al.*, "Analysis and optimization of nonlinear carrying performance of hydrostatic ram based on finite difference method and Runge–Kutta method," *Advances in Mechanical Engineering*, vol. 11, no. 6, pp. 1–12, 2019,

[56] L. Cai *et al.*, "Carrying capacity analysis and optimizing of hydrostatic slider bearings under inertial force and vibration impact using finite difference method (FDM)," *Journal of Vibroengineering*, vol. 17, no. 6, pp. 2781–2794, 2015.

[57] X. C. Zhu *et al.*, "Analysis on dynamic characteristics of closed hydrostatic guideway throttled by capillary," *Applied Mechanics and Materials*, vol. 607, pp. 594–599, 2014,

[58] NYPAN LJ *et al.*, "Optimization of conical hydrostatic bearing for minimum friction," *ASME, Pap 71-Lub19*, no. APRil, 1971.

[59]   Z. F. Liu et al., "Thermal and tilt effects on bearing characteristics of hydrostatic oil pad in rotary table," *Journal of Hydrodynamics*, vol. 28, no. 4, pp. 585–595, 2016,

[60]   L. Lu et al., "Research on static stiffness of hydrostatic bearing using fluid-structure interaction analysis," *Procedia Eng*, vol. 29, pp. 1304–1308, 2012,

[61]   A. W. Yacout et al., "The surface roughness effect on the hydrostatic thrust spherical bearing performance (part 2 of 5, clearance type of bearings)," *American Society of Mechanical Engineers, Tribology Division, TRIB*, no. April, 2006,

[62]   A. W. Yacout, "The surfacse roughness effect on the hydrostatic thrust spherical bearings performance (part 3 of 5, recessed clearance type of bearings)," *ASME International Mechanical Engineering Congress and Exposition, Proceedings (IMECE)*, vol. 9, no. September, pp. 431–447, 2007,

[63]   S. C. Sharma et al., "Influence of recess shape on the performance of a capillary compensated circular thrust pad hydrostatic bearing," *Tribol Int*, vol. 35, no. 6, pp. 347–356, 2002,

[64]   N. Singh et al., "Performance of membrane compensated multirecess hydrostatic/hybrid flexible journal bearing system considering various recess shapes," *Tribol Int*, vol. 37, no. 1, pp. 11–24, 2004,

[65]   S. C. Sharma et al., "Performance of hydrostatic/hybrid journal bearings with unconventional recess geometries," *Tribology Transactions*, vol. 41, no. 3, pp. 375–381, 1998,

[66]   M. Fillon et al., "Effect of presence of lifting pocket on the THD performance of a large tilting-pad thrust bearing," *Friction*, vol. 3, no. 4, pp. 266–274, 2015,

[67]   M. Wasilczuk et al., "Field tests on hydrodynamic and hybrid operation of a bidirectional thrust bearing of a pump-turbine," *Lubricants*, vol. 5, no. 4, 2017,

[68]   A. Bouzidane et al., "Equivalent stiffness and damping investigation of a hydrostatic journal bearing," *Tribology Transactions*, vol. 50, no. 2, pp. 257–267, 2007,

[69]   F. Canbulut et al., "Experimental analysis of frictional power loss of hydrostatic slipper bearings," *Industrial Lubrication and Tribology*, vol. 61, no. 3, pp. 123–131, May 2009,

[70]   O. J. Bakker et al., "Recess depth optimization for rotating, annular, and circular recess hydrostatic thrust bearings," *J Tribol*, vol. 132, no. 1, pp. 1–7, 2010,

[71]   F. E. Horvat et al., "Comparative experimental and numerical analysis of flow and pressure fields inside deep and shallow pockets for a hydrostatic bearing," *Tribology Transactions*, vol. 54, no. 4, pp. 548–567, 2011,

[72]   F. Shen et al., "Three-dimensional pressure- and shear-driven flow phenomena in a circular recess of a hydrostatic rotary table," *Proc Inst Mech Eng C J Mech Eng Sci*, vol. 228, no. 6, pp. 989–1004, 2014,

[73]   Y. Zhang et al., "Research on influence of cavity depth on load capacity of heavy hydrostatic bearing in variable viscosity condition," *Adv Mat Res*, vol. 129–131, pp. 1181–1185, 2010,

[74]   Z. TIAN et al., "Static Properties of Hydrostatic Thrust Bearing Considering Couple Stress," *DEStech Transactions on Engineering and Technology Research*, no. 3rd/amma, pp. 29–33, 2017,

[75]   X. Yu et al., "Numerical Simulation of the Effects of Recess Depth on Dynamic Effect of Hydrostatic Thrust Bearing," vol. 31, no. Acn, pp. 1–5, 2013,

[76]   J. P. Shao et al., "Effect of recess depth on lubrication performance of annular recess hydrostatic thrust bearing by constant rate flow," *Industrial Lubrication and Tribology*, vol. 70, no. 1, pp. 68–75, 2018,

[77]   M. Helene et al., "Numerical study of the pressure pattern in a two-dimensional hybrid journal bearing recess, laminar, and turbulent flow results," *J Tribol*, vol. 125, no. 2, pp. 283–290, 2003,

[78]   Y. Q. Zhang et al., "Analysis on influence of oil film thickness on temperature field of heavy hydrostatic bearing in variable viscosity condition," *Adv Mat Res*, vol. 239–242, pp. 1418–1421, 2011,

[79]   J. P. Shao et al., "Influence of load capcaity on hydrostatic journal support deformation in finite element calculation," *Journal of Central South University of Technology*, vol. 15, no. 2, pp. 245–249, 2008,

[80]   T. Liu et al., "Thermal simulation modeling of a hydrostatic machine feed platform," *International Journal of Advanced Manufacturing Technology*, vol. 79, no. 9–12, pp. 1581–1595, 2015,

[81]   Y. Q. Zhang et al., "Deformation analysis of hydrostatic thrust bearing under different load," *Applied Mechanics and Materials*, vol. 494–495, pp. 583–586, 2014,

[82]   P. H. Zhang et al., "Relationship between roundness errors of shaft and radial error motions of hydrostatic journal bearings under quasi-static condition," *Precision Engineering-Journal of the International Societies For Precision Engineering and Nanotechnology*, vol. 51, pp. 564–576, 2018,

[83]   A. K. Rajput et al., "Combined influence of geometric imperfections and misalignment of journal on the performance of four pocket hybrid journal bearing," *Tribol Int*, vol. 97, pp. 59–70, 2016,

[84]   P. Sapirstein, "Accurate measurement with photogrammetry at large sites," *J Archaeol Sci*, vol. 66, no. February 2016, pp. 137–145, 2016,

[85]   R. A. J. Van Ostayen et al., "A mathematical model of the hydro-support: An elasto-hydrostatic thrust bearing with mixed lubrication," *Tribol Int*, vol. 37, no. 8, pp. 607–616, 2004,

[86]   K. Ahmed et al., "Mechanical, swelling, and thermal aging properties of marble sludge-natural rubber composites," *International Journal of Industrial Chemistry*, vol. 3, no. 1, pp. 1–12, 2012,

[87]   T. Susanto *et al.*, "Thermal aging properties of natural rubber-styrene butadiene rubber composites filled with modified starch from Dioscorea Hispida Denst extract prepared by latex compounding method," *AIP Conf Proc*, vol. 2049, 2018,

[88]   B. Moon *et al.*, "Study on the aging behavior of natural rubber/butadiene rubber (NR/BR) blends using a parallel spring model," *Polymers (Basel)*, vol. 10, no. 6, 2018,

[89]   M. Michalec *et al.*, "A review of the design and optimization of large-scale hydrostatic bearing systems," *Engineering Science and Technology, an International Journal*, no. February, 2021,

[90]   C. Xu *et al.*, "Analysis of the Static Characteristics of a Self-Compensation Hydrostatic Spherical Hinge," *J Tribol*, vol. 137, no. 4, pp. 1–5, 2015,

[91]   M. Wodtke *et al.*, "Large hydrodynamic thrust bearing: Comparison of the calculations and measurements," *Proceedings of the Institution of Mechanical Engineers, Part J: Journal of Engineering Tribology*, vol. 228, no. 9, pp. 974–983, 2014,

[92]   W. U. R. Rehman *et al.*, "Fuzzy logic-based intelligent control for hydrostatic journal bearing," *Measurement & Control*, vol. 52, no. 3–4, pp. 229–243, 2019,

[93]   K. E. Rydberg, "Hydraulic accumulators as key components in energy efficient mobile systems," *Proceedings of the 6th International Conference on Fluid Power Transmission and Control, ICFP 2005*, no. February, pp. 124–129, 2005.

[94]   M. Xian-ting, "Review of the present status of hydraulic accumulator," *Applied Mechanics and Materials*, vol. 246–247, pp. 629–634, 2013,

[95]   W. Latas *et al.*, "A new type of hydrokinetic accumulator and its simulation in hydraulic lift with energy recovery system," *Energy*, vol. 153, pp. 836–848, 2018,

[96]   D. Buhagiar *et al.*, "Modelling of a novel hydro-pneumatic accumulator for large-scale offshore energy storage applications," *J Energy Storage*, vol. 14, pp. 283–294, 2017,

[97]   D. Zhao *et al.*, "Design of a new hydraulic accumulator for transient large flow compensation," *Energies (Basel)*, vol. 12, no. 16, 2019,

[98]   M. Dai *et al.*, "The application study of accumulator used in hydraulic system of 20MN fast forging machine," *Applied Mechanics and Materials*, vol. 80–81, pp. 870–874, 2011,

[99]   Y. Zhang *et al.*, "Viscosity influence research on load capacity of heavy hydrostatic bearing," *Key Eng Mater*, vol. 450, pp. 63–66, 2011,

[100]   Y. Q. Zhang *et al.*, "Analysis on influence of oil film thickness on temperature field of heavy hydrostatic bearing in variable viscosity condition," *Adv Mat Res*, vol. 239–242, pp. 1418–1421, 2011,

[101]   M. Gohara *et al.*, "Static characteristics of a water-lubricated hydrostatic thrust bearing using a membrane restrictor," *Tribol Int*, vol. 75, pp. 111–116, 2014,

[102]   E. L. Xu *et al.*, "Investigations on the applicability of hydrostatic bearing technology in a rotary energy recovery device through CFD simulation and validating experiment," *Desalination*, vol. 383, pp. 60–67, 2016,

[103]   J. Alcántara *et al.*, "Marine atmospheric corrosion of carbon steel: A review," *Materials*, vol. 10, no. 4, 2017,

[104]   H. Rippel, *Cast Bronze Hdyrostatic Bearing Design Manual*. Cleveland: Cast Bronze Institute, inc., 1969.

[105]   A. M. Loeb *et al.*, "Determination of optimum proportions for hydrostatic bearings," *ASLE Transactions*, vol. 1, no. 2, pp. 241–247, Jan. 1958,

AUTHOR'S PUBLICATIONS

Related to the PhD study topic

MICHALEC, M., P. SVOBODA, I. KŘUPKA, M. HARTL. A Review of the Design and Optimization of Large-scale Hydrostatic Bearing Systems. Engineering Science and Technology, an International Journal, 2021, vol. 24, issue 4, s. 936-958. ISSN: 2215-0986. [IF = 5.7] (Author's contribution 70 %)

MICHALEC, M., V. POLNICKÝ, J. FOLTÝN, P. SVOBODA, P. ŠPERKA, J. HURNÍK. The prediction of large-scale hydrostatic bearing pad misalignment error and its compensation using compliant support. Precision engineering. Elsevier, 2022, vol. 75, 67-79. doi:10.1016/j.precisioneng.2022.01.011 [IF = 3.6] (Author's contribution 40 %)

MICHALEC, M., J. HURNÍK, J. FOLTÝN, P. SVOBODA. Contactless measurement of hydrostatic bearing lubricating film using optical point tracking method. *Proceedings of the Institution of Mechanical Engineers, Part J: Journal of Engineering Tribology*, 2022, vol. 237, issue 1, 1-9. https://doi.org/10.1177/13506501221108138. [IF = 2.0] *(Author's contribution 40 %)*

MICHALEC, M., T. DRYML, D. JAVORSKÝ, L. SNOPEK, M. ČUPR, J. FOLTÝN, P. SVOBODA. Assembly error tolerance estimation for large-scale hydrostatic bearing segmented sliders under static and low speed conditions. *Machines*. MDPI, 2023, vol. 11, p.14. doi:10.3390/machines11111025 [IF = 2.6] *(Author's contribution 54 %)*

MICHALEC, M., M. ONDRA, M. SVOBODA, J. CHMELÍK, P. ZEMAN, P. SVOBODA, R. L. JACKSON. A novel geometry optimization approach for multi-recess hydrostatic bearing pad operating in static and low-speed conditions using CFD simulation. *Tribology Letters*. Elsevier, 2023, vol. 71, issue 52, p.14. doi:10.1016/j.precisioneng.2022.01.011 [IF = 3.2] *(Author's contribution 65 %)*

Other publications

MICHALEC, M., P. SVOBODA, I. KŘUPKA, M. HARTL. Tribological behaviour of smart fluids influenced by magnetic and electric field – A review. *Tribology in Industry*, 2018, vol. 40, issue 4, pp. 515-528. ISSN: 0354-8996. [Citescore = 2.6] *(Author's contribution 65 %)*

MICHALEC, M., P. SVOBODA, I. KRUPKA, M. HARTL a A. VENCL. Investigation of the tribological performance of ionic liquids in non-conformal EHL contacts under electric field activation. *Friction*, 2020, 8(5), 982-994. ISSN 2223-7690. Available from: doi:10.1007/s40544-019-0342-y [IF = 7.4] *(Author's contribution 65 %)*

VENCL, A., M. KANDEVA, E. ZADOROZHNAYA, P. SVOBODA, M. MICHALEC, A. MILIVOJEVIĆ a U. TRDAN. Studies on structural, mechanical and erosive wear properties of ZA-27 alloy-based micro-nanocomposites. *Proceedings of the Institution of Mechanical Engineers, Part L: Journal of Materials: Design and Applications*, 2021. https://doi.org/10.1177/1464420721994870. [IF = 2.5] *(Author's contribution 5 %)*

ČERNÁK, M., M. MICHALEC, M. VALENA, M. RANUŠA. Inlet shape optimization of pneumobil engine pneumatic cylinder using CFD analysis. Journal of Physics: Conference Series 1935. *Journal of Physics: Conference Series*, 2021. ISBN: 1742-6588. [Citescore = 0.7] *(Author's contribution 30 %)*

APPLIED RESEARCH OUTCOMES

POLNICKÝ, V.; M. MICHALEC, P. SVOBODA, D. ROBENEK: Experimental stand for testing hydrostatic bearing of large structures in the area of special equipment. Laboratory A3/109 IMID, FME, BUT, Technická 2896/2 616 69 Brno, functional sample (2020).

SVOBODA, P.; V. POLNICKÝ, M. MICHALEC, D. ROBENEK. Brno University of Technology, Antonínská 548/1, 60200 Brno, Veveří, Czech Republic, IČ: 216305 (40 %) Bosch Rexroth, spol. s r.o., Těžební 1238/2, 62700 Brno, Černovice, Czech Republic (60 %): Device for testing the operating conditions of segmental axial hydrostatic bearings, utility model (2022).

FOLTÝN, J.; POLNICKÝ, V.; MICHALEC, M.; SVOBODA, P.; MARTINEK, J.; ROBENEK, V.: Experimental device 3PAD; Hydrostatic bearing with feedback film thickness control. Laboratory B2/305 IMID, FME, BUT, Technická 2896/2 616 69 Brno, functional sample (2023).

CURRICULUM VITAE

Ing. Michal Michalec

Date and place of birth: 14.8.1995, Trenčín, Slovakia

Education:
- **2019 - 2024** – Doctoral study at Institute of Machine and Industrial Design, Faculty of Mechanical Engineering, Brno University of Technology.
  Dissertation thesis topic: Improvement of large-scale hydrostatic bearings.
- **2017 - 2019** – Master study at Institute of Machine and Industrial Design, Faculty of Mechanical Engineering, Brno University of Technology.
  Master's thesis topic: Tribological characteristics of smart fluids.
- **2014 - 2017** – Bachelor study at Faculty of Mechanical Engineering, Brno University of Technology.
  Bachelor's thesis topic: Experimental rig for study of lubricant film in compliant contact of oil seal using fluorescence technique.
- **2010 - 2014** – Gymnázium Ľudovíta Štúra v Trenčíne, grammar school.

Awards:
- **2018** – Excellent internship student (ADIENT, Trenčín, Slovakia)
- **2021** – IMID Director prof. Martin Hartl award for excellent doctoral study results

TEACHING AND SCIENTIFIC ACTIVITIES

Lectures:
- Engineering Drawing Fundamentals – 1K-A (English)
- Engineering Drawing – 2K-A (English)

Seminars:
- Engineering Drawing Fundamentals – 1K-A (English)
- Engineering Drawing Fundamentals – 1K (Czech)
- Engineering Drawing – 2K-A (English)
- Engineering Drawing – 2K (Czech)
- Project Management – ZRS (Czech)
- Mechanical Design Project – ZIP (Czech)
- Research and Development Project – ZKR (Czech)

Participation in scientific projects:
- **2019 – 2022** – National Competence Center of Mechatronics and Smart Technologies for Engineering (TN01000071)
- **2021 - 2023** – Research and development of turntable hydrostatic bearing based on adaptive regulation loops (FW03010357).

Internships:
- **7/2023** University POLITEHNICA of Bucharest, Romania
  (Modelling of bearing performance based on experimental data)
- **1/2023** University of Maribor, Slovenia
  (Mesh improvement techniques in numerical modelling)
- **1/2022 - 5/2022** Auburn University, USA
  (CFD numerical modelling of bearing interfaces, lubricating layers)
- **8/2021** INSA Lyon, France
  (FEM numerical modelling of fluid films)
- **6/2021** TU Wien, Austria
  (Materials and surface treatment, texturing)
- **7/2018 - 8/2018** ADIENT Technological Centre Trenčín, Slovakia
  (Design of a mechanism)

Language skills:
- Slovak (native), Czech (bilingual), English (C1/C2), German (A2/B1)

Scientific activities:
- Numerical and experimental modelling of hydrostatic lubrication
- Rheology, friction and wear measurement and evaluation
- Machine design and structural analysis of components
- Hydraulic and pneumatic system design

ABSTRACT

This dissertation thesis deals with the experimental and numerical study of large-scale hydrostatic bearings. Such bearings are used to carry and manipulate large structures precisely and smoothly, as the sliding surfaces of the bearing are completely separated by an externally pressurized lubricating film. Since its first official introduction in 1852, extensive research has been conducted on performance improvement. Nonetheless, the researchers primarily focused on hydrostatic bearings of small sizes, while very little research focused on larger dimensions of this type of bearing. In such cases, completely different challenges arise, which are connected with higher energetic demands, the bearing parts manufacturability, transportation and assembly. Manufacturing errors, improper bearing alignment or non-optimal design can worsen the bearing performance, and even cause its malfunction. This thesis aims to introduce performance and safety improvements into large-scale hydrostatic bearing design methodology. The bearing performance improvement is performed using a numerical model of the fluid domain that is validated using experimental and theoretical data. This study presents a completely new approach based on optimizing multiple geometric parameters of the hydrostatic bearing pad independently. The safety improvement is performed purely experimentally. The attention is aimed at pad and slider misalignment, and their influence on the bearing performance. Moreover, the self-aligning ability of the pad using compliant support is examined. The experimental part was carried out using testing hydrostatic bearing consisting of two pads with full diagnostics. As the results indicate, the proposed optimization methodology of geometric parameters of a hydrostatic bearing can improve the bearing performance by as much as 20 %. The investigation of misalignment effects on the performance shows certain range, within the bearing can still operate safely, while compliant support can extend this range. This study presents original research expanding the knowledge of large-scale hydrostatic bearing systems towards better performance and higher safety.

ABSTRAKT

Táto dizertačná práca sa zaoberá experimentálnym a numerickým štúdiom veľkorozmerných hydrostatických ložísk. Takéto ložiská sa používajú na presné a plynulé polohovanie veľkých konštrukcií, pretože klzné plochy ložiska sú úplne oddelené externe tlakovaným mazacím filmom. Od jeho prvého oficiálneho predstavenia v roku 1852 prebehol rozsiahly výskum na zlepšenie výkonnosti. Napriek tomu sa výskumníci primárne zameriavali na hydrostatické ložiská malých rozmerov, zatiaľ čo len veľmi malá časť výskumu sa zameriavala na väčšie rozmery tohto typu ložísk. V takýchto prípadoch vznikajú úplne iné výzvy, ktoré sú spojené s vyššou energetickou náročnosťou, výrobou dielov ložísk, dopravou a montážou. Výrobné chyby, nesprávne zarovnanie ložísk alebo neoptimálna konštrukcia môžu zhoršiť výkonnosť ložiska, čo môže viesť až k jeho poruche. Cieľom tejto dizertačnej práce je predstaviť vylepšenia výkonu a bezpečnosti do rozsiahlej metodiky návrhu hydrostatických ložísk. Zlepšenie výkonu ložiska sa vykonáva pomocou numerického modelu oblasti tekutiny, ktorý je overený pomocou experimentálnych a teoretických údajov. Táto štúdia predstavuje úplne nový prístup založený na nezávislej optimalizácii viacerých geometrických parametrov hydrostatickej ložiskovej kapsy. Zlepšenie bezpečnosti sa vykonáva čisto experimentálne. Pozornosť je zameraná na nesúosovosť klzných plôch kapsy a bežca a ich vplyv na výkon ložísk. Okrem toho je skúmaná schopnosť samo-vyrovnávania podložky s použitím poddajnej podstavy. Experimentálna časť bola vykonaná pomocou testovania hydrostatického ložiska pozostávajúceho z dvoch káps s plnou diagnostikou. Ako ukazujú výsledky, navrhovaná metodika optimalizácie geometrických parametrov hydrostatického ložiska môže zlepšiť výkon ložiska až o 20 %. Skúmanie vplyvov nesúosovosti na výkonnosť ložiska ukazuje určitý rozsah, v rámci ktorého môže ložisko stále bezpečne fungovať, zatiaľ čo poddajná podpora môže tento rozsah ešte predĺžiť. Táto štúdia predstavuje originálny výskum rozširujúci poznatky o rozsiahlych hydrostatických ložiskových systémoch smerom k lepšiemu výkonu a vyššej bezpečnosti.